



SRTTU

Journal of Computational and Applied Research  
in Mechanical Engineering

jcarme.sru.ac.ir

JCARME

ISSN: 2228-7922

Research paper

## State of the art in friction stir welding and ultrasonic vibration-assisted friction stir welding of similar/dissimilar aluminum alloys

Satish Chinchankar\* and Vaibhav S. Gaikwad

Department of Mechanical Engineering, Vishwakarma Institute of Information Technology, Pune, Maharashtra, 411048, India

### Article info:

#### Article history:

Received: 06/10/2020  
Revised: 03/03/2021  
Accepted: 04/03/2021  
Online: 06/03/2021

#### Keywords:

UVeFSW,  
Hybrid welding,  
Aluminum alloy,  
Tool geometry,  
Post-weld treatments,  
Optimization techniques.

#### \*Corresponding author:

[satish.chinchankar@viit.ac.in](mailto:satish.chinchankar@viit.ac.in)

### Abstract

Researchers have worked on many facets of joining of similar/dissimilar aluminum alloys using different joining techniques and came up with their own recommendations. Friction Stir Welding (FSW) is widely preferred for joining aluminum alloys being an economical alternative to produce high-quality welds. However, obtaining high strength welded joints without the detrimental and visible effects still needs attention considering the effect of hybrid FSW techniques, tool material and geometry, process parameters (tool rotation, welding speed, and plunge depth), and post welding treatments. This study presents the state of the art with the authors' own inferences on the evaluation of FSW performances in terms of joint tensile strength, fatigue strength, corrosion resistance, residual stresses, microstructure, and microhardness. This study also presents attempts made by the researchers on modeling and parametric optimization of FSW to finding scope for application of advanced optimization techniques and development of predictive models for mechanical properties of welded joints. This study emphasizes more studies required on the comparative evaluation of FSW performance with the application of ultrasonic frequency combinedly or individually on advancing and retreating sides of plates.

## 1. Introduction

Friction stir welding (FSW), a novel solid-state welding process invented by Wayne Thomas at TWI in 1991, is the most significant development in the joining of dissimilar metals. FSW is a green technology due to its energy efficiency, environment friendliness, and versatility. FSW overcomes many of the

problems associated with traditional joining techniques. FSW produces welds of high quality in difficult-to-weld materials such as aluminum and is a fast-becoming process of choice for manufacturing lightweight transport structures for boats, trains, and airplanes [1].

FSW has been widely used in the manufacturing of rocket-fuel tanks. These tanks are made up of high-strength aerospace aluminum alloys which

are difficult to join by conventional welding techniques. FSW offers significant cost gains by reducing production times especially in case of difficult to join materials. FSW process utilizes a non-consumable rotating welding tool to generate frictional heat and plastic deformation at the welding location. Due to low welding temperature, mechanical distortion is practically eliminated, with minimal Heat Affected Zone (HAZ), and an excellent surface finish. The FSW process is effective on flat plated, cylindrical components and even parts of irregular thickness [2].

The quality of the FSW joints largely depends on the process parameters such as rotational speed, welding speed, and different tool pin profiles, namely cylindrical (straight, taper, and threaded) and square (straight and tapered). Several studies concluded that joining of high strength aluminum alloys and dissimilar metals using FSW has become an economical alternative to the conventional fusion welding process. However, microstructural characteristics and mechanical behavior of joints depending on the FSW process variables play a vital role in the successful application of the FSW in Aerospace and Space applications. Recently, friction stir processing (FSP) was developed for microstructural modification of metallic materials [1].

In FSW, a joint between sheets or plates is produced in a ‘solid state’ using a combination of rotation and translation motion to a non-consumable rotating tool along the line of a joint as shown in Fig. 1.

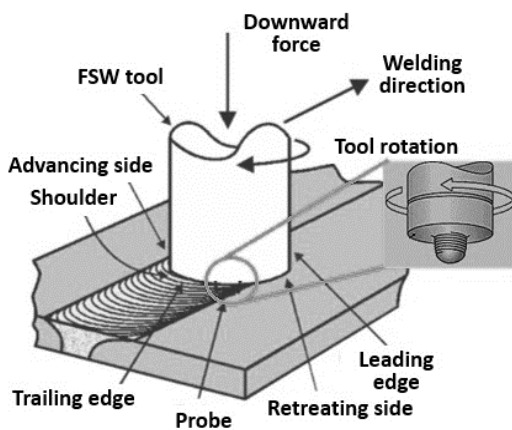


Fig. 1. Friction stir welding process [1].

The heating is accomplished by friction between the tool and the workpiece and plastic deformation of the workpiece. The localized heating softens the material around the pin and a combination of tool rotation and translation leads to movement of material from the front of the pin to the back of the pin. Because of various geometrical features of the tool, the material movement around the pin can be quite complex. During the FSW process, the material undergoes intense plastic deformation at elevated temperature, resulting in the generation of fine and equiaxed recrystallized grains. The fine microstructure in friction stir welds produces good mechanical properties.

Welding of aluminum alloys using conventional arc welding is difficult due to the formation of the oxide layers, especially at weld nugget and shrinkages during the solidification process. Researchers have worked on many facets of joining similar and dissimilar aluminum alloys using different joining techniques and came up with their own recommendations [2-8]. Researchers have observed marginal improvement in the mechanical properties of the welded joint with conventional welding techniques.

On the other hand, researchers have observed minimum distortions and lower residual stresses in weld nugget while joining Al alloys with FSW [3-4]. And, hence, FSW is widely preferred for joining aluminum alloys being an economical alternative to produce high-quality welds. However, obtaining high strength welded joints without the detrimental and visible effects still needs attention considering the effect of hybrid FSW techniques, tool material and geometry, process parameters (tool rotation, welding speed, and plunge depth), and post welding treatments. This study presents state of the art on the evaluation of FSW performances while joining similar and dissimilar aluminum alloys to give proper attention to various researcher works.

This study also presents attempts made by the researchers on modeling and parametric optimization of FSW with a view to finding scopes for the application of advanced optimization techniques and the development of predictive models for mechanical properties of welded joints. Initially, the literature available on different welding techniques to join similar

and dissimilar aluminum alloys is presented with their deliberations.

A comprehensive literature review on FSW and its variant processes, hybrid FSW (Hybrid-FSW), is presented with a view to understanding the applicability of the process for difficult-to-join materials and to have a joint with better mechanical properties. Further, attempts made by various researchers to comparatively evaluate welding performance with FSW and hybrid-FSW are presented. Researchers' works on FSW/hybrid-FSW considering different tool materials and geometries are also presented as a selection of tool geometry and tool material that are very crucial and play an important role in obtaining quality joint with better mechanical properties

Further, researchers' works to evaluate the welding performance are presented to understand the effect of FSW process parameters and joining technique (conventional or hybrid) on joint tensile strength, fatigue strength, microhardness, microstructure, corrosion resistance, and residual stresses. The joint efficiency and joint strength play a key role especially in aerospace and defense applications. Most researchers have observed enhancement in the mechanical properties and behavior of microstructure with post-weld treatments.

With this view, studies available on post-weld treatments, their procedure, and important results are presented. Further, attempts made by researchers to model and optimize performance measures are presented with a view to having more understanding of the parametric effect during FSW of aluminum alloys. Finally, important observations from various researchers' works during FSW of similar and dissimilar aluminum alloys are summarized and concluded.

## 2. Welding techniques: Al alloys

Continuing efforts being taken by automakers and original equipment manufacturers to reduce the weight of the vehicle weight by using lightweight materials without scarifying the strength requirements. A significant benefit in terms of higher fuel economy and lower CO<sub>2</sub> emissions can be obtained with low weight vehicle. Increasing demands for high strength

lightweight vehicles have triggered for obtaining joints from similar and dissimilar metals. However, obtaining high strength joints with similar and dissimilar metals using conventional fusion welding methods is challenging and has process limitations.

Researchers have worked on many facets of joining similar and dissimilar metals using various welding techniques as shown in Fig. 2. Automobile manufacturers started preferring lightweight materials such as aluminum, copper, magnesium, and their alloys for various automobile panels and structures to reduce the weight of the vehicle with a view to improving fuel economy. At present, aluminum consumption is 180 kg/vehicle and predicted to increase up to 250 kg/vehicle by 2025. This necessitates the joining of similar and dissimilar metals for many components and assemblies. However, joining and repairing automobile parts made up of similar and dissimilar alloys are going to be a challenging task [2].

It is widely reported that friction stir welding and its variant processes are the most efficient way to join similar and dissimilar metals. FSW being a solid-state process involves lower values of temperature as compared to Metal Inert Gas Welding (MIG) and Tungsten Inert Gas Welding (TIG) processes. Lower process temperature resulted in lower heat-affected zone and hence, minimum alterations in material properties as compared to MIG and TIG joining processes. Moreover, defects such as porosity, lack of wetting, hot cracking, strength reduction, distortion, and residual stresses are significantly less in FSW joints in comparison to MIG and TIG welding processes [3-7].

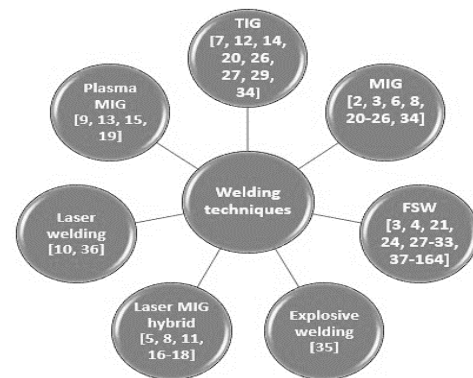


Fig. 2. Attempts made by researchers to join aluminum alloy(s) using various joining techniques.

A group of researchers employed hybrid joining processes (a combination of two welding processes) such as laser beam welding (LBW) and MIG, MIG and TIG, double-sided TIG and MIG, LBW and MIG, plasma welding and MIG, large spot Nd: YAG LBW and MIG with a view to obtaining improved joint characteristics. However, joints obtained with hybrid processes showed lower mechanical and chemical properties due to the fusion of end surfaces as

against properties observed with FSW joints [1-2, 8-16]. Several attempts have been made by researchers to join similar/dissimilar aluminum alloys using different joining techniques. Attempts made by various researchers and their findings while joining similar and dissimilar metals especially aluminum alloys using different joining techniques are shown in Table 1.

**Table 1.** Welding techniques and their deliberation.

Joining technique(s) and work material(s)	Deliberations
Fusion welding and aluminum alloy [2]	Hot tears, solidifying cracks, porosity, distortion, and melt through were observed in weld bead which drastically reduced fatigue strength and mechanical properties of joints.
FSW and MIG, and 6082-T6 and 6061-T6 alloys [3]	Lower hardness values and fatigue lives observed in the MIG welded specimens in comparison to FSW specimens.
FSW and aluminum and stainless-steel joint [4]	The main cause of defects in the weld zone was the detachment of steel particles in the aluminum matrix. Their simulation study revealed an increase in tool rotational speed and offset through the steel side could generate more steel particles.
Laser and MIG hybrid brazing-fusion welding and 6013-T4 aluminum alloy and galvanized steel [5]	The authors observed a reduction in joint strength due to the formation of an intermetallic compound (IMC) layer with a thickness of 2-4 μm.
Pulse metal inert-gas welding and wrought 6061-T6 and cast A356-T6 aluminum alloy [6]	The joint strength observed 83% that of the 6061-aluminum alloy. Lower values of microhardness were observed due to the larger heat affected zone (HAZ). The tensile strength of the joint was observed to vary with the travel speed and found optimum at 12 mm/s.
Ultrasonic-assisted TIG welding and pure aluminum [7]	Welding current and ultrasound amplitude were observed as key process parameters that affects the grain fragmentation. Welding current showed linear and ultrasound amplitude showed a non-linear relationship with the grain fragmentation.
MIG welding and laser MIG welding (hybrid welding) and copper joint [8]	Hybrid welding showed smaller areas of heat affected zone and fusion zone as compared to MIG. It was also noted that the tensile strength of the hybrid joint was 74 % and MIG has 69 % that of the base material.
Plasma-MIG hybrid (PMH) welding and Al 5083 plates and Al5183 [9]	The higher deposition rate and lower porosity were observed during the joining of dissimilar alloys with Plasma-MIG hybrid welding.
Laser beam welding and die-cast aluminum alloy AC-AlSi9MnMg [10]	Electromagnetic field-assisted laser beam welding showed a reduction in pores and better weld surface smoothness, almost by 75% as that of joints obtained by LBW.
Laser-MIG hybrid welding and 7075-T6 aluminum alloy [11]	The fatigues fracture surfaces of the welded joint showed the gas porosities and dimples.
Double-pulsed variable polarity gas tungsten arc welding and AA2219 aluminum [12]	Joining process was observed with an improved stirring effect which resulted in equiaxed grain as well as microstructure and consistent microhardness in the welded joint.
Hybrid plasma-MIG Welding and Al5083 alloy [13]	The plasma-MIG welding method was observed to help in improving the corrosion resistance of Al5083 welding joints.
TIG welding and 2219 aluminum [14]	The authors observed fewer pores in the welded joint when using direct current electrode negative-TIG technique and coarser grain structure with variable polarity-TIG.

---

Plasma-MIG welding and 5A06 aluminum alloy [15]	Plasma gas flow rate was observed as more dominant than welding voltage, welding speed, wire feed rate, and plasma current.
Plasma arc welding and plasma MIG welding, and cryogenic aluminum alloys [16]	The authors observed minimum smut formation at higher values of current and significant effect by nozzle diameter on surface defects.
Fiber laser-MIG hybrid welding and 5083 aluminum alloy [17]	No significant benefit in microstructure and mechanical properties of the welded joint was observed with helium, mix of helium and argon shielding gases during hybrid welding.
Laser-MIG hybrid welding and Fe36Ni invar alloy [18]	Authors observed a more stirring effect in the molten pool with higher values of current resulted in pores in the weld region and uneven HAZ.
Plasma-MIG welding and aluminum alloy [19]	The metastable spray transfer and projected transfer modes were observed as optimal modes in terms of stability of the electronic signal, droplet transition, weld appearance, and weld penetration.
MIG and TIG welding, and AA5052 aluminum alloy and Q235 low-carbon steel [20]	The authors observed a thicker IMC layer with a higher MIG voltage and thinner IMC layer at higher welding speeds.
FSW and MIG welding, and 6082 aluminum alloy [21]	The corrosion rate of the FSW joint was less than those of the parent material and MIG joint.
MIG arc brazing-fusion welding and galvanized steel and 5052 aluminum alloy [22]	The authors developed a modified flux mixture to improve the butt joint performance. The modified flux produced better weld appearance and improved the spreadability of filler metal.
Bypass-current MIG (BC-MIG) welding-brazing and AA6061/Ti-6Al-4V [23]	The authors observed a reduction in the heat input and an increase in the melting efficiency of Al filler wire with BC-MIG welding-brazing. Average joint strength was observed as 180 MPa, about 91% of Al base metal.
FSW and 2024 aluminum alloy [24]	Developed a monitoring system using surface images to detect the defective weld with 95% accuracy. Their study observed lower tensile strength with irregular weld surface appearance.
MIG welding followed by friction stir welding and 6082-T651 aluminum alloy [25]	Authors observed that FSW assisted in improving the fatigue strength of the MIG welded joints and useful in lowering porosity defects and lack of wetting as observed with MIG welded joints.
MIG-TIG double-sided arc welding-brazing and 5052 aluminum alloy/mild steel [26]	Authors observed excellent weld appearance, joint with higher tensile strength and thin IMC layer without any cracks with MIG-TIG double-sided arc welding brazing while joining dissimilar joint of 5052 aluminum alloy and mild Steel.
FSW and TIG welding and AA2014 aluminum alloy [27]	Authors observed finer Al-matrix grains at the nugget zone of the FSW joint in comparison to larger Al matrix grain size along with coarse precipitates in the HAZ of the TIG weld joint. Finer grains showed more passivation and improved corrosion resistance of the FSW joints. On the other hand, larger grains observed at TIG weld reduced the passivation and hence, showed poor corrosion resistance. Moreover, the authors observed higher microhardness of the FSW joint than the TIG weld joint.
FSW and AA1050 aluminum alloy [28]	The authors observed that the insertion of the brass interlayer at the joint seam increased the FSW joint efficiency up to 90% against observed 60% without interlayer at the joint. However, no significant benefit observed in joint efficiency by the Authors when using zinc and copper interlayer at the joint seam.
FSW and TIG welding and Al-Mg-Si alloy 6082 [29]	Authors observed that friction stir welded joint has higher static and dynamic strength in comparison to MIG-pulse and TIG welds.
FSW and TIG welding and AA 2024-T3 [30]	The authors observed higher microhardness and corrosion resistance with friction stir welded joint in comparison to TIG welds.
FSW and GTAW and aluminum 6061 [31]	Authors observed equiaxed grains with FSW as against dendritic structure at the welded region by GTAW. FSW joint also showed improved corrosion resistance against GTAW joint.

---

FSW and Al 5083-H321 and 316L stainless steel [32]	Authors found that tool traverse speed has a significant effect on the mechanical properties of the joint produced. The joints tensile strength was observed to decrease due to the formation of the tunnel and void defects with an increase in the tool traverse speed from 160 to 200 mm/min.
FSW and aluminum and stainless steel [33]	The formation of the IMC layer was observed with the use of a cutting pin, especially when the insertion of the pin was less than the thickness of plates to be joined.
MIG/TIG double-side arc welding-brazing and Ti6Al4V and 5A06 [34]	Welded joints with higher tensile strength due to lower IMC layer (thickness of 1–2 μm) were observed with MIG/TIG double-side arc welding-brazing as against MIG weld joints.
Explosive welding and 6082-T6 aluminum alloy and AISI 304 stainless steel [35]	Explosive welding showed better performance when steel was used as a base plate. It is reported that flyer material used should have higher thermal conductivity, higher melting point, and higher specific heat.
Laser welding and aluminum 6014 [36]	Weld produced with oscillation had higher tensile strength as that of a triple spot. However, laser welding induced porosity in the joint.
FSW and 7050-T7451 aluminum alloys [37]	Authors found an increase in average hardness and fatigue life with the laser shock peening (LSP) process to FSW welds. With the LSP process, compressive residual stresses were produced in the weld nugget zone, thermo-mechanically affected zone (TMAZ), and HAZ.

From the literature reviewed, it has been observed that TIG, MIG, laser welding, a combination of TIG and MIG, a combination of plasma and MIG, and FSW were mostly used for joining of similar and dissimilar aluminum alloys. However, amongst the various techniques, FSW is considered to be the most efficient technique for joining similar and dissimilar aluminum alloys. The joints obtained with FSW showed equiaxed grain structure, higher corrosion resistance, and higher fatigue strength as compared with the joints obtained with available joining techniques.

With this, the authors of the present paper conclude that FSW and its variant processes are the best choices to effectively join similar and dissimilar aluminum alloys. However, researchers are continuously working in this domain using a combination of different joining techniques; hybrid welding with a view to obtaining better mechanical properties. With this view, in the next section, researchers' work on hybrid FSW during the joining of aluminum alloys are presented to understand the comparative evaluation of welding performance and process applicability for difficult-to-join materials.

### 3. Hybrid friction stir welding

From the available literature on the joining of aluminum alloys (Pl. refer Section 1 and 2), FSW has evolved as the most efficient technique

to join similar and dissimilar aluminum alloys. However, researchers are continuously working in this domain using a combination of different joining techniques; hybrid welding, with a view, to make the process applicable for difficult-to-join materials and to have a joint with better mechanical properties. A group of researchers attempted to join similar and dissimilar metals using the FSW technique combining assistance of ultrasonic vibrations, plasma, high tool rotation, etc. with a view to obtaining higher joint efficiency.

Most of the researchers carried FSW with the ultrasonic frequency at generally 20 Hz along the weld line [38]. Liu et al. [39] investigated the FSW with ultrasonic vibrations for joining aluminum alloy. Their experimental investigations concluded that ultrasonic assistance improved the quality of the weld, enhanced the joint mechanical properties, and increased the heat input at the localized areas. Xu et al. [40] investigated the joining of Mg/Ti by ultrasonic-assisted welding brazing. They reported that ultrasonic assistance lowered the grain size to 50 μm which was initially 200 μm. Refinement in the grain improved the corrosion resistance and improved the tensile strength of the joint by 18%. Liu et al.'s [41] investigation on the material flow and plastic deformation during ultrasonic-assisted FSW concluded that ultrasonic energy had a significant effect on flow velocity, the volume of deformed material, and strain/strain rate.

Shakil et al. [42] investigated the microstructural and mechanical properties of dissimilar joints (stainless steel with aluminum alloy) using ultrasonic welding. Lei et al. [43] observed better overall properties of the welded joint of magnesium alloy by ultrasonic-assisted laser welding. Their results revealed that the porosity of weld joint declined to 0.9% from 4.3% and the tensile strength of the joint improved by 7%. Kumar et al. [44], in their review article on the application of ultrasonic vibrations, concluded that ultrasonic vibrations improved mechanical properties and material flow at the joint and reduced tool wear.

Wu et al. [45] investigated the joining of AA 2024-T3 using ultrasonic vibration-assisted FSW (UVEFSW). Their study showed that the application of ultrasonic vibrations reduced the stress concentration at the bonding region. Moreover, the fatigue strength of the UVEFSW joint was observed to increase by 96% in comparison to the fatigue strength of the FSW joint. Zhong et al. [46] investigated the material flow and temperature distribution assisting ultrasonic vibrations during FSW of AA6061-T6 to AA2024-T3. Their study observed a reduction in torque requirement and axial force by giving ultrasonic vibrations. Further, observed improved material flow resulted in defect-free joint.

Liu et al. [47] investigated the effect of ultrasonic vibrations to FSW joint with a view to eliminate the tunnel defects. Their study showed that the tunnel defect normally observed at the lower rotating speed can be avoided by having higher welding speed (feed) or with the smaller axial force. Gao et al.'s [48] experimental work while joining of Al6061-T6 concluded that net strain component is slightly higher in joints obtained with UVEFSW resulted in refinement of the grain in comparison to FSW. Liu et al.'s [49] study observed defects free Mg/Al joints with UVEFSW as ultrasonic vibrations assisted in breaking inter metallic compound layer (IMC) resulted in improvement of the tensile strength of the joint.

Meng et al.'s [50] investigation also confirmed that FSW assisted with ultrasonic vibrations helped in the elimination of IMC and metal adhesion to pin resulted in improved material flow and hence, better tensile strength (115

MPa) of Mg/Al joint. Padhy et al. [51] found a better recrystallization process, higher deformation characteristics at the nugget zone, and refined grains while joining Al6061-T6 by assisting ultrasonic vibrations to FSW than the FSW. Liu et al. [52] also observed better material flow in the UVEFSW process as compared to the FSW process. Gao et al. [53] investigated the joining of AA2024-T3 by UVEFSW. Their experimental work noticed that the effect of ultrasonic vibrations started decreasing gradually from the center and was more effective at the stir zone. They observed improved grain refinement in the immediate deformation zone and stir zone and higher ductile fracture in the case of UVEFSW than FSW.

Padhy et al. [54] also observed the formation of sub-grain and the maximum at the center of the stir zone while joining aluminum alloy by using the UVEFSW process. Ji et al. [55] investigated the joining of AZ31 magnesium alloy and 6061 aluminum alloy using UVEFSW. Their experimental observations concluded that ultrasonic assistance that improved the material flow led to the interlocking of Mg and Al and improved the mechanical properties of the joint due to the breaking of IMC into smaller particles. Lv et al.'s [56] experimental study while joining magnesium alloy to aluminum alloy using UVEFSW observed the formation of lower IMC, better tensile properties, and improved fracture morphology of Mg/AL joint with ultrasonic frequency as compared to FSW. They also observed ductile fracture of the joint with UVEFSW as against brittle fracture observed with joint obtained with FSW.

Shi et al. [57] developed a mathematical model for UVEFSW and observed a significant role of ultrasonic softening in improving the mechanical properties of the joint and obtaining defects free joint. In another study, Shi et al.'s [58] numerical simulation of UVEFSW showed that superimposing the ultrasonic improves strain rate, material flow, and enlarges the deformation. Kumar [59] observed during the joining of 6063 aluminum alloy with UVEFSW that the ultrasonic frequency assisted in the generation of heat in the stir zone improved the tensile strength and hardness and lowered the transverse force required by the tool.

Thoma et al. [60] observed a clean nugget zone while joining aluminum and steel using UVeFSW. However, no significant difference was observed by them in corrosion resistance in joints obtained by FSW and UVeFSW. Lv et al.'s [61] investigation on UVeFSW while joining Mg/Al alloy concluded that ultrasonic vibration reduced the IMC and improved the mechanical properties especially the tensile strength of the joint even at lower spindle speed. An increase in tensile strength even at lower spindle speed could be attributed to an increase in the temperature at the stir zone due to ultrasonic vibrations which resulted in better material flow. An experimental setup of hybrid FSW is shown in Fig. 3.

And the comparison of microstructure and top surface obtained using FSW and UVeFSW are shown in Fig. 4 and Fig. 5

It can be seen that the application of ultrasonic frequency while FSW assisted in a rise in temperature along the weld line improved the flow velocity of material, hence resulted in lowering porosity, refined grain size, and better quality of weld appearance [39, 46, 52, 53, 60]. Researchers are continuously working on using a combination of different joining techniques; hybrid welding, with a view, to make the process applicable for difficult-to-join materials and to have a joint with better mechanical properties. Researchers have observed improvement in welding performance using hybrid FSW techniques such as ultrasonic vibration-assisted FSW (UVeFSW). Hybrid UVeFSW improved the flow of material along the weld line in FSW in comparison to conventional FSW resulting in improved surface finish, tensile strength, grain size, and reduction in the IMC layer.

Almost all the works reported observed better mechanical properties of the weld joint with UVeFSW in comparison to joint properties obtained with conventional FSW. However, further studies are required to comparatively evaluate FSW performance with the application of ultrasonic frequency on advancing and/or retracting side of the plates, individually and simultaneously.

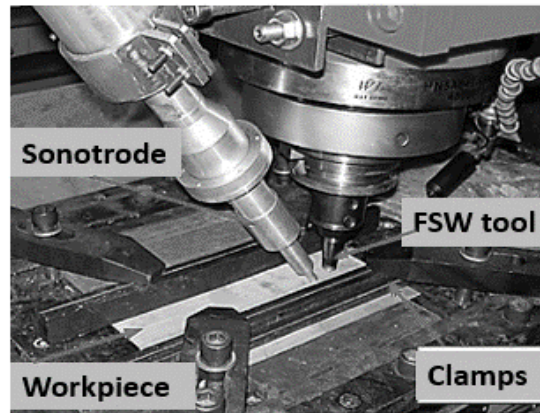


Fig. 3. Experimental set up for hybrid UVeFSW [38].

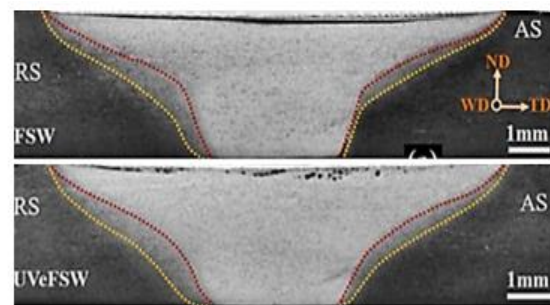


Fig. 4. Macrographs of FSW and UVeFSW of AA2024-T3 joint [53].

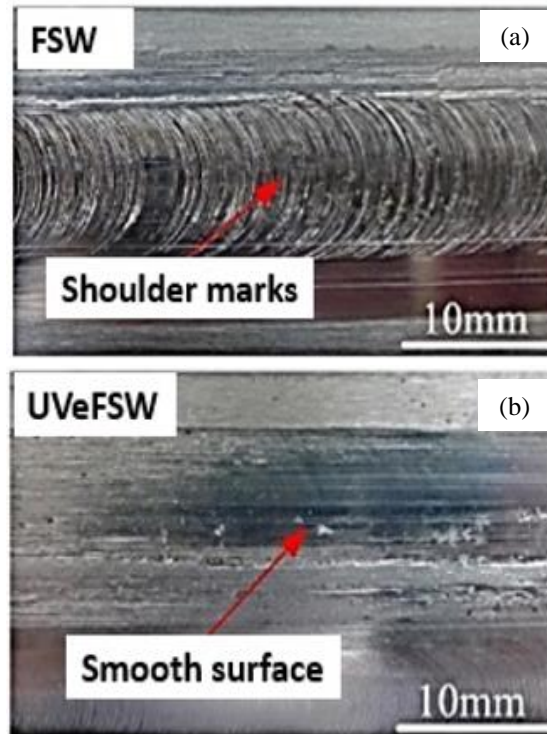


Fig. 5. Top surface appearance of (a) FSW and (b) UVeFSW of 6061-T6 aluminum alloy and AZ31B magnesium alloy joint [49].



With the joining technique, the selection of the tool geometry is also very crucial as it significantly affects the mechanical properties of welded joint and joint efficiency. With this view, in the next section, the researchers' works on FSW of aluminum alloys with different tool geometries are presented with a view to understanding the effect of tool geometries on weld formation and mechanical properties of the welded joint.

#### 4. Tool material and geometry

It is very well demonstrated that the desired performance of any processes largely depends on the selection of their process parameters. In FSW, process parameters such as tool rotation, feed rate, tool plunge depth, tool material and geometry, and workpiece material significantly affect process performance. In FSW, a specially designed tool is used to get the required joint. This tool, because of its rotation and translation along the direction of the weld, provides thermomechanical action to get the required joining. The tool consists of the shoulder and the pin. The tool's shoulder transfers the axial load on the work surface and the rotating pin stirs and transfers the plasticized material along the length of the joint.

The selection of the tool shoulder size and geometry (shape) is very important as they significantly affect the mechanical properties of welded joint and joint efficiency. In this section, researchers' works on FSW of aluminum alloys with different tool geometries are presented with a view to understanding the effect of tool geometries on weld formation and mechanical properties of the welded joint.

A lot of efforts were made by researchers to investigate the effect of tool geometry, especially the hybrid tool geometry on FSW performance. It is reported that welding with hybrid tool geometry was performed at a faster rate and joint with improved mechanical properties and better material flow was obtained [62]. Rai et al. [62] in their review article, reported that tungsten-based and PCBN-based alloys are the best tool materials for obtaining quality joints with better mechanical properties. Mastanaiah et al. [62] while joining AA2219-T6 using a hybrid pin profile, observed improved

mechanical properties and the material flow against the conical geometry tool. They found 26% better strength for the joint with a hybrid tool. Hou et al.'s [64] investigation while joining aluminum alloys observed defect-free joint with the dual-pin profile as against single pin profile. Moreover, higher ultimate tensile strength (UTS) for the joint was observed with dual-pin profile in comparison to the single pin profile.

Zhao et al. [65] investigated the effect of tool geometry during the joining of TRIP steel and AA6061 and observed higher tensile strength of about 85% as that of the aluminum base metal when using a larger tool. Beygi et al. [66] investigated the effect of tool geometry, namely pyramidal, threaded cylindrical, and threaded conical while joining Al/Cu. Their study concluded that the threaded conical pin tool geometry produced better joint in terms of improved material flow and higher tensile strength. This could be attributed to more contact area of the pin led to higher plasticized material flow. Hajideh et al. [67] carried joining of polypropylene sheet and polyethylene using FSW with different tool pin profiles, namely squared, threaded cylindrical, straight cylindrical and triangular. Their study observed better mechanical properties with the threaded cylindrical tool which could be attributed to laminar material flow as against non-laminar flow observed with other tool profiles.

Chen et al. [68] carried material deformation analysis of the rectangular tool pin profile. Their study observed a significant reduction in the volume of the deforming material and a drop in temperature by about 10°C as compared with conventional FSW. Piccini et al. [69] optimized tool geometry while joining Al-steel using friction stir spot welding (FSSW). Their study showed a variation in IMC thickness with tool geometry. They observed the smallest IMC thickness of 5 µm with "C" shape tool geometry. Kumar et al.'s [70] investigation on tool geometry observed better quality of FSW joint with a frustum-shaped rounded-end pin. They observed that the grain size of 5 to 20 µm in the stir zone increased with an increase in the shoulder diameter. A maximum joint efficiency of about 92% was observed with shoulder and pin diameter of 20 mm and 6 mm respectively. Garg et al. [71] also investigated the

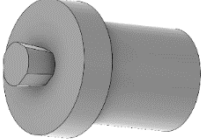
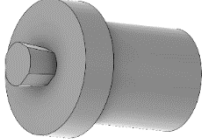

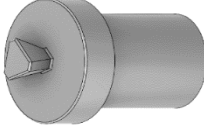

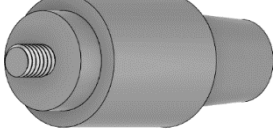
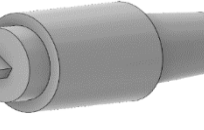
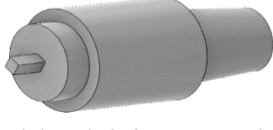
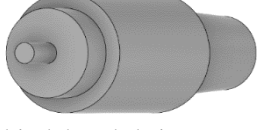
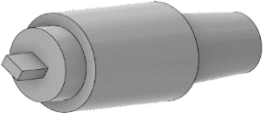
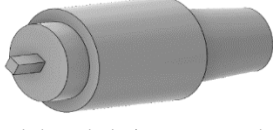
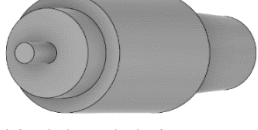
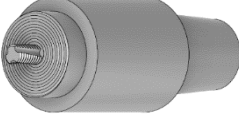
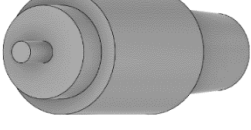
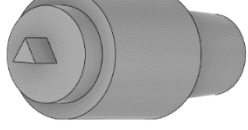
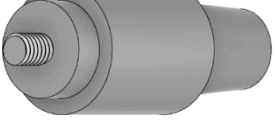
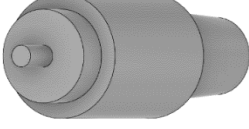
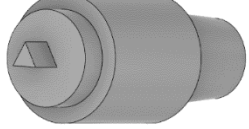
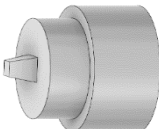
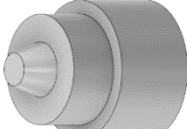
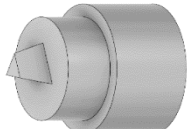
performance of friction stir spot welding (FSSW) with different pin and tool geometries. Amongst different pin lengths (0.4 mm, 0.2 mm, and pin-less (0 mm)) investigated by them, the

maximum lap shear strength and asymmetric strain distribution were observed with the pin-less profile. They also observed an increase in the stir zone with an increase in the pin diameter.

**Table 2.** Different tool materials and geometries used while joining aluminum alloys by FSW.

Workpiece and tool materials [Ref]	Tool geometry(ies)	Research finding(s)
7020-T6 Al and high carbon steel tool [73]	a) Straight circular pin, concave shoulder b) Tapered cylindrical pin with three flats, concave shoulder	Uniform material flow was observed with both tool geometries.
Al5754 and H13 steel tool [74]	a) Cylindrical pin, concave shoulder b) Triangular pin, concave shoulder	A continuous hook profile with a cylindrical pin and upward hook with a triangular profile observed. Static strength with a triangular pin was twice as that of a cylindrical pin.
6111-T4 aluminum alloy and H13 steel tool [75]	Triflat threaded pin, flat shoulder	Their study observed pin length to be 0.7-1 mm and insulated anvil reduced the lap shear strength by 15% with a rise in the temperature by 45°C in the bottom sheet.
Commercial aluminum and tempered steel tool [76]	a) Straight threaded pin, flat shoulder b) Flat pin, flat shoulder	Comparatively evaluated tensile strength with two tool geometries. Their study observed higher tensile strength with a flat pin profile tool against a straight threaded tool.
AA7075-T651, AA606 and HSS tool [77]	a) Square pin, flat shoulder b) Cylindrical pin, flat shoulder c) Triangular pin, flat shoulder	Investigated the effect of various tool pin profile on the tensile strength of joint. Their study observed better tensile strength with the square pin profile tool.
A6082-T6 and hot die steel tool [78]	Conical threaded pin, concave shoulder	Their study observed better material flow with a concave shoulder geometry tool.
6082-T6 aluminum alloy and HSS tool [79]	a) Cylindrical threaded pin, grooved spiral shoulder b) Triflute pin, grooved spiral shoulder c) Cylindrical pin, flat shoulder	Investigated the effect of different tool geometries on weld quality and tensile strength. Their study observed better tensile strength with triflute pin profile as compared to other tool geometries investigated in their work.
AA2024-T351 D2 and tool steel [80]	a) Triangular pin, flat shoulder b) Cylindrical threaded pin, flat shoulder	Investigated the effect of tool geometries on mechanical properties and found better results with a triangular pin profile as against threaded cylindrical tool.
AA7039 and AISI 316 tool [81]	a) Circular V-threaded pin, flat shoulder b) Circular V-threaded pin, 1 mm flat and 7° taper shoulder c) Circular V-threaded pin, 2 mm flat and 7° taper shoulder	Maximum tensile strength, tensile toughness, and % elongation observed with circular V-threaded pin and shoulder with 1 mm flat and 7° taper. Whereas lower values were observed with a circular V-threaded pin and fully flat shoulder.
65032 aluminum and High carbon steel tools [82]	a) Taper cylindrical pin, flat shoulder b) Taper triangular pin, flat shoulder c) Taper square pin, flat shoulder	The authors observed the highest joint efficiency of 73 % with a taper cylindrical pin as against 43% observed with a taper triangular pin.

**Table 3.** 3-D images of different tool geometries used while joining aluminum alloys by FSW.

Straight circular pin, concave shoulder [73]	Tapered cylindrical pin three flats, concave shoulder [73]	Cylindrical pin, concave shoulder [74]
		
Triangular pin, concave shoulder [74]	Triflat threaded pin, flat shoulder [75]	Straight threaded pin, flat shoulder [76]
		
Flat pin, flat shoulder [76]	Square pin, flat shoulder [76]	Cylindrical pin, flat shoulder [77]
		
Triangular pin, flat shoulder [77]	Conical threaded pin, concave shoulder [78]	Cylindrical threaded pin, grooved spiral shoulder [79]
		
Triflute pin, grooved spiral shoulder [79]	Cylindrical pin, flat shoulder [79]	Triangular pin, flat shoulder [80]
		
Cylindrical threaded pin, flat shoulder [80]	Circular V-threaded pin, 1 mm flat and 7° taper shoulder [81]	Circular V-threaded pin, 2 mm flat and 7° taper shoulder [81]
		
Taper square pin, flat shoulder [82]	Taper cylindrical pin, flat shoulder [82]	Taper triangular pin, flat shoulder [82]
		

Ullegaddi et al.'s [72] investigations while joining AA-6082 T6 with concentric shoulder, flat shoulder, scroll shoulder tool profiles observed better joint efficiency with tapered threaded tool pin with the concave shoulder. Researchers' works on FSW of aluminum alloys with different tool geometries are shown in Table 2 and their 3-D images are shown in Table

3 with a view to understanding the effect of tool geometries on weld formation and mechanical properties of the welded joint.

It is reported that the selection of tool geometry and tool material is very crucial and play an important role in obtaining quality joint with better mechanical properties. From the literature reviewed, authors observed that tools with flat

shoulder and circular pin profile were most commonly used to join similar and dissimilar aluminum alloys. However, further investigations are required to obtain optimum pin profile and shoulder shape for better mechanical properties of the welded joint.

It is seen that with the use of a square or triangular pin profile more material is removed from the advancing side and will get deposited on the retreating side resulting in the poor quality of joint. And, hence, it is suggested to prefer a conical threaded tool with a flat shoulder for the better quality of joint while FSW of similar and dissimilar aluminum alloys. However, the authors observed limited research on the effect of hybrid tool geometry (a combination of two different geometries) on weld formation and mechanical properties of welded joint.

It has been widely reported that FSW process parameters prominently affect joint tensile strength, fatigue strength, microhardness, microstructure, corrosion resistance, and residual stresses and discussed in the next section.

**5. Performance measurements**

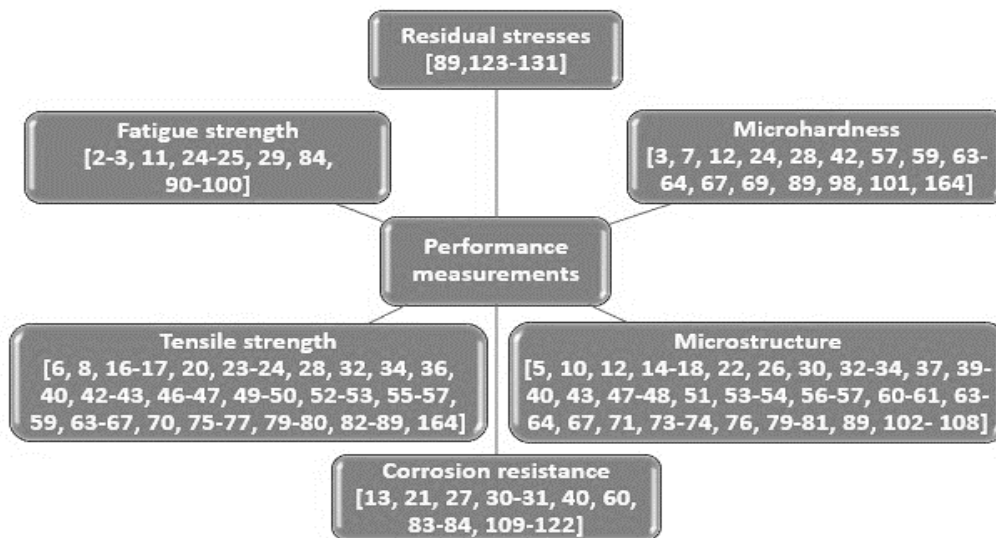
Sufficient efforts have been made by the researchers to improve the performance of the friction stir welded joints of similar and

dissimilar aluminum alloys using hybrid welding techniques. In this section literature available on the performance of FSW joints of aluminum alloys in terms of tensile strength, fatigue strength, microhardness, microstructure, corrosion resistance, and residual stresses are presented and discussed.

*5.1. Tensile strength*

Aluminum alloys find several applications in the aircraft structures, vehicles, pressure vessels, TV towers, etc. However, joint strength and efficiency are key aspects when fabricated from similar and/or dissimilar aluminum alloys. In the design of the aircraft structures, attempts are always aimed towards maximizing the tensile strength of the welded joint. The important features to be considered while designing next-generation aircraft are the lighter, stiffer, stronger, and use of more damage tolerant material. Hence, tensile strength needs to be evaluated for the aluminum joint [83, 84].

This section presents the attempts made by various researchers in obtaining and improving the tensile strength of FSW joints of aluminum alloys using hybrid welding techniques. Attempts made by researchers to evaluate performance during FSW of similar and dissimilar aluminum alloys is shown in Fig. 6.



**Fig. 6.** Attempts made by researchers to evaluate performance during FSW of similar and dissimilar aluminum alloys.

Hamed et al. [85] investigated the mechanical properties and microstructure during the friction stir welding of dissimilar AA5086 and AA7075 alloys. During their study, the focus was on the effect of post-weld heat treatment and heat input on the mechanical properties and microstructure of the welded joint. They concluded that the amount of AA7075 increased in the stir zone with an increase in heat input if the weld was performed without a heat sink. Also, tensile strength observed by them was more with the use of heat sink and found to increase as heat input increased. Furthermore, grain size was observed to be fine in the stir zone if the weld was made using the heat sink and coarse in case of without heat sink.

Rao et al. [86] investigated the tensile behavior and mechanical properties of 5083 aluminum alloy FSW joints. Micro-tensile and indentation tests were applied to determine the local mechanical properties in a friction stir welded joint. Their results of micro-tensile tests agreed with results seen for hardness distribution at the welded joint. Further, their study showed that the Al5083 FSW joint fractured at the retreating side of the HAZ even though the strength measured was lower at the advancing side. It was due to the crack initiated at the retreating side because of the presence of a root flaw.

Sabari et al. [87] evaluated the mechanical properties of AA2519-T87 aluminum alloy joints made by FSW and underwater FSW (UWFSW). Their study observed that underwater FSW joint exhibited higher tensile strength (271 MPa) and higher joint efficiency (60%) than conventional FSW joint. Huang et al. [88] performed micro-FSW of Al-6061 material having a sheet thickness of 0.5 mm. During their study, they investigated the effect of process parameters such as plunging depth and rotational velocity on the sound surface formation and tensile properties of the weld joint. They found an optimum plunging depth of 0.05 mm and the maximum tensile strength of the joint as 217 MPa.

Fathi et al. [89] comparatively evaluated the tensile strength for conventional FSW and water-cooled FSW and found that FSW performed with water as a cooling medium

improved the tensile strength of aluminum 6061-T6 joint by 16%.

From the literature reviewed, it has been observed that the tensile strength of the welded joint is predominantly affected by FSW parameters such as tool shoulder diameter, pin geometry, welding speed, tool rotational speed, plunging depth, and axial force. Welding techniques such as conventional FSW, hybrid FSW, and welding with cooling medium also affected the tensile strength of the welded joint. It is seen that post-weld heat treatments and heat input play a major role in deciding the mechanical properties and microstructure of the welded joint. It has been observed that FSW performed with water as a cooling medium improved the tensile strength of the welded joint in comparison to strength obtained with conventional FSW.

## 5.2. Fatigue strength

Fatigue strength is a key aspect while designing an aircraft structure. It is the maximum stress that is taken by the material for a certain number of cycles without fracture. The measurement of fatigue strength of aluminum welded joint is also important as crack initiation starts due to stress concentration at the fasten holes [84]. This section presents the attempts made by various researchers in evaluating the fatigue strength of welded joints.

Fig. 7 shows the schematic diagram of the standard test specimen to be used while evaluating the fatigue strength of the welded joint. And Table 4 shows the parameters namely frequency and load ratio used by various researchers during the fatigue test of welded joints of aluminum alloys.

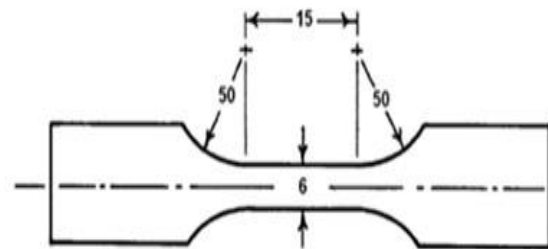


Fig. 7. Fatigue test specimen [90].

**Table 4.** Specifications for evaluation of fatigue life of welded joints for aluminum alloys.

Authors	Workpiece material	Specifications	
		Frequency (Hz)	Max to Min load ratio
Moreira et al. [3]	6082-T6 and 6061-T6 aluminum alloy	7–26	0.1
Bahrami et al. [90]	Aluminum 7075 alloy	300	-1
Moghadam et al [91]	2024-T351 aluminum alloy	10	--
Liu et al. [92]	AlZnMgCu alloy	100	0.1
Rodriguez et al. [93]	AA6061 and AA7050	5	-1
Vysotskiy et al. [94]	Al–Mg–Si alloy	50	0.1
Guo et al. [95]	6061-T651 and 5083-H321 aluminum alloy	10–15	0.1
Cavaliere et al. [96]	2024-7075 aluminum alloy	70	0.1

Bahrami et al. [90] investigated the effect of SiC reinforcement during FSW of aluminum 7075 alloys. They carried out experiments at a transverse speed of 40 mm/min and tool rotation of 1200 rpm with and without insertion of SiC nanoparticles. Their work revealed that the presence of SiC nanoparticles improved the fatigue life of the component. Their study observed fatigue life (number of cycles to fracture) as 25310 for SiC included specimen as against 17300 for specimens without SiC reinforcement. Moghadam et al. [91] observed that transverse speed and tool rotational speed significantly influenced the development rate of fatigue crack and fracture while FSW of 2024-T351 aluminum. Rodriguez et al. [93] investigated the low cycle fatigue performance of welded joints of AA6061 and AA7050. Their work revealed a decrease in amplitude of plastic strain and an increase in stress amplitude when the fatigue test performed at strain amplitude greater than 0.3% and a frequency of 5 Hz. Their study reported no tangible difference in fatigue life of welded joints of similar alloys and that of dissimilar alloys.

Guo et al. [95] investigated the fatigue performance of FSW of 5083-H321 and 6061-T651 joints. In their work, intentional defects were kept in the welded joints to evaluate their effects on the fatigue life of the component. Their work observed higher fatigue life for properly welded butt joint. However, the fatigue life of the component was observed to decrease with kissing bond defect at the joint. Cavaliere et al. [96] investigated the fatigue behavior of FSW aluminum 2024-7075 alloys. They performed a

fatigue tests at 25 kN at a frequency of 70 Hz. Moreira et al. [3] investigated the fatigue life of MIG welded and FSW specimen of 6082-T6 and 6061-T6 aluminum alloys. Their study observed higher fatigue life for the FSW component in comparison to that of MIG welded specimen. They also observed higher fatigue life for the FSW joint of a 6082-T6 specimens than that of the FSW joint of 6061-T6. Yang et al. [97] investigated the high cycle fatigue in double-sided FSW of 6082Al-T4 aluminum alloy. Their study observed fatigue life distribution for the three layers (top, middle, and bottom) approximately the same tendency with the same fatigue limit of 110 MPa and the same fatigue ratio of 0.49. They observed that lower- and middle-layers specimen failed in HAZ whereas upper layer specimen showed abnormal failure in the nugget zone.

Kumar et al. [98] investigated microhardness and fatigue life of the dissimilar FSW joint of AA5083 and AA6063 alloys. Fatigue tests were performed at a load of 22 Kg and for life cycles of  $2 \times 10^6$  and at completely reversible loading conditions. Their study observed failure of a component at lower values of cycles when stress value was very high. Deng et al. [99] investigated the crack initiation in FSW aluminum 7075 alloys. They observed that the crack initiation started at thermo-mechanically affected zone on the advancing side at life cycles of  $1 \times 10^6$  and  $5 \times 10^7$  whereas failure originated at the life of  $5 \times 10^7$  and  $1 \times 10^9$ . Milcic et al. [100] investigated the fatigue behavior of FSW of Al2014-T351 alloy. Their experimental investigation showed higher fatigue strength

when welding performed at tool rotation of 750 rpm and welding speed of 116 mm/min as against tool rotation of 750 rpm and welding speeds of 73 mm/min and 150 mm/min.

From the literature reviewed, it is seen that the fatigue tests were performed mostly by varying frequency and load ratios. It has been observed that the fatigue strength of FSW joints mostly affected by parameters such as stress ratio, residual stress, weld defect, tool geometry, welding speed, and tool rotational speed. It is seen that the presence of SiC nanoparticles improved the fatigue life of the component. The fatigue life of the component was observed to decrease with kissing bond defect at the joint. It has been also observed that joints obtained using FSW provided better fatigue lives in comparison to joint obtained using conventional fusion-welded joints.

### 5.3. Microhardness and microstructure

The microhardness test is a test wherein the applied load is less than 10 N. Microhardness test measures the quality of the weld with respect to the base material. It also gives the analysis of heat affected zone and hence, is widely used for evaluating the quality of weld during the joining of aluminum alloys [101]. Fathi et al. [89] investigated the comparative evaluation of microhardness of aluminum 6061-T6 joint obtained using FSW and FSW with water as a cooling medium. Their study showed the improved value of microhardness almost by 12.5% for FSW when performed with water as a cooling medium. Kumar et al. [98] observed the microhardness of the weld zone lies between the base metals investigated during FSW of AA5083 and AA6063.

Microstructural observations of the welded joint reveal the quality of joints. It is reported that the finer the grain size, the higher the quality of the joint, whereas the coarse microstructure worsen the quality of the joint. Various attempts have been made by researchers to correlate the physical and mechanical properties of the welded joint with the microstructural observations of the FSW joint [102]. Fathi et al. [89] analyzed the microstructure of FSW and FSW with water as a cooling medium while joining aluminum 6061-T6. They observed that

using water as a cooling medium during FSW decreased the HAZ and refined the grains resulted in improving the tensile strength and hardness of the joint.

Leon et al. [103] observed that an increase in peak temperature (400-500°C) with intense plastic deformation influenced microstructural evolution in the stirred zone during the joining of aluminum alloys using FSW. Their investigation when compared with traditional fusion welding showed several advantages like low residual stress and fine recrystallized grains with FSW. The observed microstructural analysis of the FSW joint showed three different zones named nugget zone, thermo-mechanically affected zone, and heat-affected zone.

Bisadi et al. [104] investigated the microstructure and plunge stage in friction stir welding of aluminum 7050 plates with a tool which has a triangular pin. Microstructural observations from their study indicated macrostructural changes in the workpiece in four different zones (stir zone, thermomechanical affected zone (TMAZ), HAZ, and base metal) with different characteristics at each zone. They observed the ultra-fine grains in the stir zone and elongated grains in the direction of material flow at the TMAZ. However, they observed the formation of the new grains in the HAZ due to static recrystallization mechanism.

Wang et al. [105] investigated the effect of water as a cooling medium during friction stir welding of H19-5083Al rolled plates. Their experimental work reported that using water as a cooling medium during FSW narrowed down the hardness zone and produced the ultrafine grain structure at the welding zone.

Ma et al. [106] studied the correlation between the properties and processing to explore electrochemical properties and microstructure of friction stir welds. Their experimental work showed improvement in pitting resistance of the FSW joint of the aluminum alloys due to laser surface melting which could be attributed to improved microstructure and phase distribution. Their study observed a homogenous layer with fine microstructures at the surface which was free from precipitates and intermetallic compounds.

Avinash et al. [107] investigated the feasibility of friction stir welding of two dissimilar

aluminum alloys namely AA2024-T3 and AA7075-T6 for their structural and mechanical properties. Their experimental work observed lower weld strength of dissimilar metal as compared to the base metal. Partial ductile fracture at weld nugget was also observed by them due to variation in thickness. The authors claimed that less frictional heat was attributed to finer grain size in the stir zone.

Moradi et al. [108] study during FSW of AA2024 and AA6061 aluminum alloys observed fine equiaxed grain. This was attributed to dynamic and static recrystallization occurred at stirred zone on advancing and retreating sides. Their study observed that the slow absorption rate of dislocations into subgrain boundaries on the advancing side resulted in an increase of continuous dynamic recrystallization in comparison to the retreating side.

From the literature reviewed, it is seen that the microhardness test is most widely used for evaluating the quality of weld during the joining of aluminum alloys. It is widely reported that the finer the grain size the higher the quality of the joint whereas the coarse microstructure worsen the quality of the joint. It has been understood that the microstructure and microhardness of the welded joint is significantly affected by the FSW process parameters.

It is seen that the microhardness is strongly dependent on the rotational speed and has been found to increase with the decrease in the rotational speed. However, the microhardness observed is slightly affected by the welding speed. Fine and equiaxed grains in the nugget zone are also most observed during the FSW process.

Microstructural analysis of the FSW joint showed three different zones named nugget zone, thermo-mechanically affected zone, and heat-affected zone. It has been observed that the rigid clamping used for holding the workpiece, high levels of deformation, and temperature generated due to friction significantly affected the material flow behavior, microstructure, and mechanical properties of the welded joint. It is seen that FSW performed with water as a cooling medium lowers heat-affected zone (HAZ) and produces ultrafine grain structure resulting in improved tensile strength, microhardness, and joint efficiency of aluminum alloys.

#### 5.4. Corrosion resistance

Aluminum alloys, especially 7XXX series is widely used in aircraft structure due to its better mechanical and physical properties. However, these alloys are susceptible to stress corrosion cracking (SCC). Aircraft structures are subjected to adverse conditions such as freezing, high loads, high temperatures, hail impact, lightning strikes, and exposure to potentially corrosive fluids such as jet fuel, lubricants, and paint strippers. These conditions are susceptible to oxidization and stress corrosion cracking and hence, evaluation of corrosion resistance of welded joints, especially joints from aluminum alloys is very crucial [83, 109].

Open circuit potential, electrochemical impedance spectroscopy and polarization curve test are preferred for the corrosion test of welded joints. Dynamic polarization, morphological analysis, and dynamic potential scanning techniques are also used by researchers to measure corrosion resistance. A group of researchers evaluated the corrosion resistance of welded joints using an electrochemical corrosion test, electrochemical potentiodynamic polarization, immersion test, and local corrosion potential measurement. This section presents the attempts made by various researchers to evaluate the corrosion resistance of welded joints considering the effect of FSW parameters, workpiece material, and tool geometry.

Chen et al. [110] studied the corrosion behavior of aluminum 7075 in various sections. Their work claimed that the heat affected zone adjacent to the nugget zone is more susceptible to corrosion. Sinhmar et al.'s [111] investigations on the corrosion behavior of FSW aluminum 2014 alloy using potentiodynamic polarization test observed higher corrosion resistance at the welded joint than that of base metal. Squillace et al. [112] investigated the pitting corrosion and microstructure for TIG welded and FSW joint of AA2024-T3 alloy. Electrochemical impedance spectroscopy and polarization curve test were performed in order to determine the tendency of pitting. Their experimental results showed pitting tendency as well as HAZ for both TIG and FSW joints and their weld bead showed the passive tendency.

Balaji et al. [113] obtained the pitting corrosion resistance of FSW AA2219 using a dynamic polarization test. In their work, they optimized the process parameters to obtain better corrosion



resistance at the welded joint. They observed better corrosion resistance at the tool rotation of 1363 rpm, welding speed of 715 mm/min, and with hexagon tool pin profile. Maggiolino et al. [114] comparatively evaluated the corrosion resistance of MIG welded and FSW joints of AA6082-T6 and AA6060-T5. The corrosion test was conducted by dipping the samples in acid salt solutions and corrosion resistance was determined using morphological analysis of the surface. Their study observed better corrosion resistance with FSW joint in comparison to the MIG welded joint. Liu et al. [115] studied the effect of laser shock peening on the FSW joint of AA7075. The dynamic potential scanning technique was used to determine the corrosion resistance. Their experimental study showed significant improvement in corrosion resistance due to laser shock peening as a post-weld treatment.

Meshram et al. [116] obtained the corrosion resistance of FSW and fusion welding of an ultra-high-strength steel and maraging steel using an electrochemical corrosion test. The test was performed in 3.5% NaCl solution and in air. Their study reported superior corrosion resistance with FSW joint as compared to corrosion resistance obtained with the fusion welded joint. Jafarlou et al. [117] investigated the effect of the tool pin profile on the FSW joint of A15086 alloys. The corrosion resistance was measured using electrochemical impedance spectroscopy tests and Tafel polarization tests. Their study found better corrosion resistance of welded joint when using square geometry as a tool pin profile. Nam et al. [118] studied the effect of traveling speed on corrosion resistance of 6061 aluminum alloy. Electrochemical tests were used to determine the corrosion resistance of the FSW joints. Their study concluded that an increase in speed improved the corrosion resistance of the joint.

Sinhmar et al. [119] investigated the effect of water cooling on the corrosion behavior of AA2014 alloy. An electrochemical potentiodynamic polarization corrosion test was used to determine the corrosion resistance of the joint. Their investigation showed better corrosion resistance with water-cooled joint in comparison to that of a natural cooled joint. In another study, Sinhmar et al. [120] obtained the

corrosion behavior of AA2014 using a potentiodynamic polarization test, immersion test, and electrochemical impedance spectroscopy. They observed better corrosion resistance with FSW AA2014 joint as compared to TIG welded joint. Gianluca et al. [121] investigated the corrosion behavior for FSW AA7075, AA6060, AA2024. During their study, they used local corrosion potential measurements to determine the corrosion resistance. Their study claims that the lower the value of hardness, the more is the corrosion potential at the anode. However, they observed no systematic relationship between process variables and corrosion resistance.

Yong et al. [122] obtained the corrosion behavior of the FSW and MIG welded joint of AA6082 alloy. In their study electrochemical impedance spectroscopy, potentiodynamic polarization curve, and scanning electron microscopy (SEM) were used to determine the corrosion behavior. They observed a higher corrosion rate with MIG welded joint as compared to that of FSW joint. SEM images of their study showed deeper pits on the MIG welded joint surface as against shallow pits were observed in the FSW joint surface.

From the literature reviewed, it is seen that the corrosion resistance of the welded joint is mostly affected by the welding process parameters, tool geometry (Pin and shoulder profile in case of FSW), and workpiece material. It has also been observed that joints obtained using FSW provided better corrosion resistance in comparison to conventional fusion-welded joints. Post-weld treatments such as laser shock peening, shot peening, etc., are also seen as better techniques to improve the corrosion resistance of the welded joint. Studies also show that heat affected zone adjacent to the weld nugget is more susceptible to corrosion

### 5.5. Residual stress

Residual stresses are the secondary stresses which exist in the component after the removal of load. It can give a positive as well as a negative effect on the welded component. Tensile residual stress gives the negative effect whereas compressive residual stress is beneficial to the welded component. Residual stresses can

be correlated with the crack initiation and fatigue life of the component; hence it is necessary to measure the residual stresses induced in the welded joint [123]. Hole drilling method, contour method, cut compliance method, laser ultrasonic technique, XRD method are various methods reported in the open literature to measure the residual stresses.

Fathi et al. [89] investigated the FSW of aluminum 6061-T6 using water as a cooling medium. Prominent results in favor of lower residual stresses at the surface (of 52 MPa) was observed in the welded joint when using water as a cooling medium during FSW as against higher residual stress (of 88 MPa) was observed in conventional FSW. Also, their study observed maximum compressive residual stress (of 71 MPa) at depth of 0.3 mm when water was used as a cooling medium. Fratini et al. [124] investigated the residual stresses induced in FSW aluminum alloys using the hole drilling method. They observed residual stresses which were negative in nature (compressive) increased with an increase in hole depth up to 1 mm. Further, their study found that the maximum residual stress induced at the border of a shoulder on the advancing side which was negative in nature on the surface and became positive in nature (tensile) with the increase in depth.

Sun et al. [125] investigated the residual stresses in the welded joint of high strength aluminum alloy using the contour method for conventional shoulder FSW and stationary shoulder FSW (SSFSW). Their study observed uniform and narrow HAZ and lower value of induced peak stress in SSFSW as against the conventional shoulder FSW. Further, they observed a narrower residual stress profile with an increase in welding speed. Schwinn et al. [126] investigated the residual stresses in tailored welded blanks of AA5028-H116 using the cut-compliance-method. Their study observed that the relative error in actual values of residual stresses is of 30% with the conventional solution.

Zhan et al. [127] investigated the residual stress measurement of FSW Al7075 alloy using a laser ultrasonic technique. Their study observed that the higher residual stress on the advancing side and its distribution was asymmetric in nature. Their study showed that welding speed

prominently influenced residual stress whereas the effect of welding feed was observed as negligible. Mouhri et al. [128] investigated the relationship between residual stresses, microstructure, and thermal aspects in joining of AA1050 using FSW. Residual stresses were measured by them at different distances from the join in advancing and retreating side using the XRD method. A higher value of residual stress was observed at a higher stir rate. Trummer et al. [129] investigated the effect of clamping force on residual forces developed during the joining of AA2198-T851 using FSW. In their investigation, the contour method was used to determine the residual stresses. Their study reported that a higher clamping force of magnitude 2500 N resulted in lower distortion and uniform distribution of residual stresses along with efficient joint.

Sun et al. [130] investigated the residual stress distribution while joining of AA7050 using FSW and stationary shoulder FSW (SSFSW). Residual stresses were measured using the contour method. Their study concluded that the downward tool force did not significantly affect the distribution of residual stress. However, lower values of tensile residual stress up to 25% was observed in SSFSW. Buglioni et al. [131] developed a numerical model to predict the residual stresses in FSW of AA7075 alloy and found numerical results of residual stresses in good agreement with the experimental results. Residual stresses, prestresses or secondary stresses are very crucial in any joining process of materials since they affect the mechanical properties of the welded joint. From the literature reviewed, it is seen that the lower values of residual stresses in FSW joint as against the fusion welded joint as the temperature do not reach the fusion value of the materials. The residual stresses are induced in the welded joint due to the higher axial force and the rigid clamping used. It is also seen that the residual stresses developed in the welded joint significantly affected by the FSW process parameters. It is understood that the investigation on the residual stress distribution in the FSW welds is very important as the presence of residual stresses influences the mechanical properties of the welded joint.

From the literature available on performance measurements, it has been understood that the FSW process parameters and joining technique (conventional or hybrid) prominently affect joint tensile strength, fatigue strength, microhardness, microstructure, corrosion resistance, and residual stresses. It is seen that FSW performed with water as a cooling medium lowers heat-affected zone (HAZ) and produces ultrafine grain structure resulting in improved tensile strength, microhardness, and joint efficiency of aluminum alloys. It is also seen that the presence of SiC nanoparticles in the microstructure increased the fatigue life of the component. Also, HAZ adjacent to the nugget zone was observed as more susceptible to corrosion. Higher residual stress on the advancing side and its distribution asymmetric in nature is reported. Residual stresses in the welded joint were observed to be prominently affected by tool rotation and negligibly with welding speed (tool traverse). It has been observed that the finer the grain size, the higher the tensile strength and fatigue strength. It has been observed that the corrosion resistance of the welded joint needs to be investigated in detail considering the effect of FSW process parameters and joining techniques. Further, post-weld treatments have shown to play a major role in deciding the mechanical properties, microstructure, and joint efficiency of the welded joint. And, hence, in the next section, the efforts made by the researchers to improve the mechanical properties using post welding treatments are discussed during FSW of aluminum alloys.

**6. Post-weld treatments**

In aerospace and defense sectors and industrial applications, joint efficiency, and joint strength especially joints from similar and dissimilar aluminum alloys play a key role. It has been widely reported that the joint efficiency and strength substantially improved using post welding treatments. In the last few years, researchers have concentrated on post-weld treatment for aluminum joints. This section discusses the efforts made by the researchers to improve the mechanical properties of FSW of aluminum alloys. Mostly shot peening and laser shock peening treatments are prominently

reported in the literature as post-weld treatments as both processes induce residual compressive stresses in the weld specimen and improve fatigue life, grain structure, and tensile strength. Fig. 8 and Fig. 9 show the schematic diagram of laser shock peening and shot peening respectively.

Amuda et al. [132] investigated the effect of cryogenic cooling and addition of element metal powder during the gas tungsten arc welding of the AISI430 FSS plate. Their study observed that both strategies refined the grain structure. However, a significant reduction in heat-affected zone (HAZ) up to 50% was observed with the addition of metal powder as against cryogenic cooling reduced HAZ up to 36%. On the other hand, the cryogenic cooling resulted in joint ductility of 80% as that of the base metal, whereas the addition of element metal powder resulted in joint ductility up to 60%. Hatamleh et al. [133] observed the effect of laser-peened, shot-peened, and cryogenic cooling on fatigue crack growth and residual stresses of FSW 2195 Al alloy.

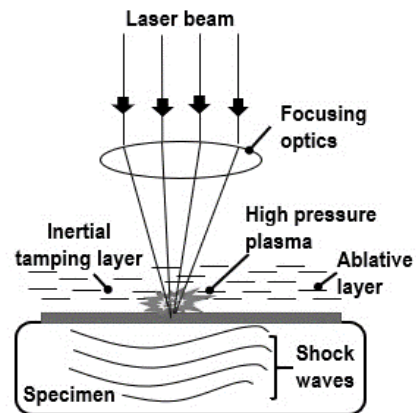


Fig. 8. Schematic diagram of laser shock peening process.

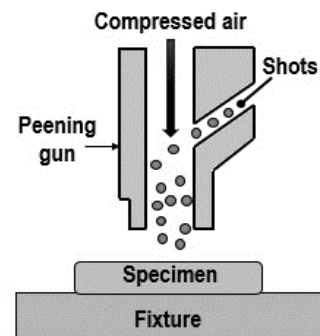


Fig. 9. Schematic of shot peening process.

Their study found that fatigue crack growth for the specimen treated with laser peened was the same as that of shot-peened and as-welded at the ambient temperature. Also, at cryogenic treatment, it was difficult to distinguish the residual stress and crack growth.

Hatamleh et al. [134] studied the effect of shot peening and laser peening on the FSW joint of 2195 Al alloy. Their study observed the improved mechanical properties with laser peening as that of shot peening. Improvement in yield strength at the nugget zone was observed around 38% when laser peening was used as post-weld treatment as against 8% improvement in yield strength at the nugget zone was observed with shot peening. Khorrami et al. [135, 136] investigated the influence of ambient and cryogenic temperature on friction stir processing of severely deformed aluminum 1050 alloy with SiC nanoparticles. Their work observed the bimodal and finer grain size when using FSW joints were used with cryogenic cooling treatment as against abnormal grain growth during the FSW.

Singh et al. [137] performed the post-weld cryogenic treatment on the FSW joint of 7075 Al alloy. Their experimental study observed that post-weld cryogenic treatment resulted in a marginal improvement in the tensile strength and hardness of the joint. Wang et al. [138] investigated the effect of low-temperature aging and cryogenic treatment on mechanical properties of FSW 2024-T351 aluminum alloy. They noted the elimination of soft zones near the heat-affected zone due to the single low-temperature aging. However, a reduction in the strength of the joint was observed due to single low-temperature aging.

Wang et al. [139] performed the cryogenic FSW of the copper joint. Their experimental work observed that the grain refinement in the nugget zone increased initially with an increase in rotational speed. However, they observed a decrease with further increase in rotational speed. Zhemchuzhnikova et al. [140] observed extensive grain refinement and improvement in the tensile strength of cryogenically treated Al-Mg-Sc-Zr FSW joint. Ferreira et al. [141] studied the effect of the glass bead and steel beads in shot peening on the weld joint. They noticed better results of fatigue and tensile strength with glass beads as against steel beads. Also, higher surface roughness was observed when using the steel beads as compared to glass beads.

A group of researchers [142] investigated the effect of laser shock peening on the microstructural properties, fatigue strength, and corrosion resistance of FSW Al alloy joints. They observed finer grain size, better corrosion resistance, and higher fatigue strength with laser shock peening treated joints as against joints without laser shock peening as a post-welding treatment. However, more studies are required in post-weld treatments to obtain better mechanical properties of the welded joint. There is also a necessity to develop predictive models for mechanical properties such as fatigue strength, residual stress, tensile strength, grain refinement, and corrosion resistance. With this view, in the next section, the researchers' attempts on optimization and modeling during FSW of aluminum alloys are presented.

## 7. FSW: Modeling and optimization

The 21<sup>st</sup> century is the era of soft computing, simulation of processes, and optimization. These techniques reduce the time and make the system efficient. In recent years, a significant emphasis has been placed by researchers on the development of predictive models for performance measures during FSW as discussed in section 5. A group of researchers also modeled the temperature distribution by developing a numerical model. Several attempts have been made by the researchers in optimization of the FSW performance. Attempts made by the researchers to model the performance measure(s) and optimization for aluminum alloy is listed in Table 5.

Shojaeefard et al. [144] developed ANN and FEA models to investigate the effect of FSW parameters, namely shoulder and pin diameter on strain rate, material flow, and welding force during the joining of AA5083 aluminum alloy.

Their study developed the correlations between the pin and shoulder diameters with the strain rate and heat-affected zone. They observed an increase in heat-affected zone with an increase in the shoulder diameter. Devaiah et al. [145] obtained optimum process parameters for % elongation and yielded strength while joining AA5083 and AA6061 by FSW. Their study considered process parameters namely, welding speed, tool tilt angle, and tool rotational speed. They observed a tool tilt angle of 20°, welding speed of 70 mm/min, and rotational speed of 1120 rpm as optimum process parameters.

**Table 5.** Researchers attempts to model and optimize FSW performance while joining aluminum alloys.

Researchers	Modeling attempt and/or optimization technique(s) used
Chen et al. [68]	Developed a CFD model for material flow analysis in retractable pin tool FSW.
Shojaefard et al. [144]	Developed a 3-D thermomechanically coupled finite element model to evaluating the effect of shoulder diameter, tool pin profiles on material flow, and strain distribution. Further, artificial neural network (ANN) model was developed by authors to correlate the HAZ, strain value with pin profile, and shoulder diameter.
Devaiah et al. [145]	Taguchi's method was used to optimize the FSW processes.
Dewan et al. [146]	Developed a model to predict tensile strength using adaptive neurofuzzy inference system (ANFIS)
Teimouri et al. [147]	Developed a model to predict tensile strength, hardness, and elongation using the Fuzzy approach and Fuzzy artificial bee colony.
Alkayem et al. [148]	Developed the ANN model to predict percentage elongation, ultimate tensile, bending angle, hardness, strength, and yield stress. Further, authors optimized the FSW processes parameters using a real-coded genetic algorithm, differential evolution, particle swarm optimization, and binary-coded genetic algorithm.
Padmanaban et al. [149]	Developed a statistical model to predict tensile strength using response surface methodology. Further, the authors optimized the processes parameters viz. tool rotational speed and welding speed using simulated annealing.
Gupta et al. [150]	Developed ANN model to predict microhardness, grain size, and tensile strength. Further, the authors optimized the FSW parameters using a hybrid approach of genetic algorithm and ANN.
Shehabeldeen et al. [151]	Developed a statistical model to predict the ultimate tensile strength of the welded joint using response surface methodology and ANFIS.
Rajamanicman et al. [152]	Developed a nonlinear thermomechanical finite element model using ANSYS for thermal distribution and residual stresses in joint.
Zhang et al. [153]	Developed a finite element model to study the flow pattern and residual stresses.
Long et al. [154]	Developed a 3-D thermal-mechanical coupled finite element model to predict temperature distribution, stress, and flow pattern.
Rao et al. [155]	Optimized the processes parameters of FSW using Taguchi's method.
Muhammad et al. [156]	Developed a model using Gibbs free energy change of formation to predict the thickness of IMC in ultrasonic enhanced FSW (UV-FSW).
Ambekar et al. [157]	Performed multi-response optimization of the FSW process using weighted principal component analysis (WPCA)- Artificial Neural Network (ANN)- particle swarm optimization (PSO) integrated approach.
Taysom et al. [158]	Developed a hybrid heat source model and first-order plus dead time (FOPDT) model to predict the temperature distribution during FSW.
Chen et al. [159]	Developed the CFD model to evaluate the material flow and temperature distribution considering the threaded pin tool.
Sabari et al. [160]	Developed a finite element model for the width of a thermo-mechanical affected zone (TMAZ) and temperature distribution.
Kim et al. [161]	Developed a model using quench factor analysis and finite element simulation with bonding criteria for prediction of hardness
Zhang et al. [162]	Developed a CFD model to obtain plastic deformation heat flux and spatial distribution of frictional heat flux.
Rzaev et al. [163]	Developed a mathematical model for temperature dynamics and to estimate the linear velocity during FSW.
Sudhagar et al. [164]	Optimized processes parameters using Grey analysis for maximizing hardness, impact strength, and tensile strength of the welded joint.

Dewan et al. [146] developed an adaptive neuro-fuzzy inference system (ANFIS) and ANN models to predict the ultimate tensile strength of the FSW joints. Their study observed lower values of mean absolute percentage error and root mean square error with the ANFIS model against the ANN model.

Teimouri et al. [147] developed a model to predict hardness, elongation, and tensile strength using a fuzzy approach. They developed a model by using the gaussian membership function with the application of artificial bee colony algorithm. Alkayem et al. [148] optimized FSW parameters using soft computing techniques such as real coded genetic algorithm, binary-coded genetic algorithm, particle swarm optimization, differential evolution coupled with ANN. Their study observed better results with differential evolution and particle swarm optimization techniques.

Padmanaban et al. [149] optimized process parameters during FSW of AA2024-AA7075 aluminum alloys using simulated annealing and response surface methodology techniques. They found joint optimum tensile strength of 271.084 MPa at a welding speed of 14.12 mm/min and tool rotation of 1087.6 rpm. Gupta et al. [150] performed multi-objective optimization using artificial intelligence during the FSW of AA6063-T6 and AA5083-O aluminum alloys. They used a hybrid approach; a genetic algorithm and ANN techniques, to predict microhardness, grain size, and tensile strength. Shehabeldeen et al. [151] optimized the tensile strength of the FSW joints of AA2024 and AA5083 aluminum alloys using RSM and ANFIS techniques. Their study observed better results with ANFIS technique. Rajamanicman et al. [152] developed a nonlinear thermomechanical finite element model to predict residual stresses during FSW of AL2014-T6. Their study observed that longitudinal stress was proportionally varying with tool rotation.

Zhang et al. [153] developed a numerical model to predict residual stresses in friction stir welding. Their study observed that longitudinal residual stresses are significantly affected with pin translational velocity as against rotational velocity. They observed an increase in energy dissipation on friction with an increase in pin angular velocity. However, they observed an

increase in the plastic dissipation and a decrease in the frictional dissipation with an increase in translational velocity.

Long et al. [154] established a three-dimensional thermal-mechanical coupled finite element model considering the tilt angle in the geometric model. The developed model was able to predict in-process thermal-mechanical state variables (e.g. temperature, flow path, and stress) during the welding and the post-welding morphology of the weld. Their study found that the tilt angle increased the peak temperature in the surrounding region of the welding tool resulted in the softening of the material. Moreover, their study observed that the tilt angle of 2° enhanced the material flow from the rear retreating side to the rear advancing side.

Rao et al. [155] optimized processes parameters for FSW of AA6061 and polycarbonate with a view to getting joint with maximum tensile strength. During their study, they considered plunge depth, welding speed, and rotational speed as process parameters. They found that plunge depth of 1.2 mm, feed of 100 mm/min and tool rotation of 1400 rpm produced the joint with the maximum tensile strength of 10.33 MPa.

Muhammad et al. [156] investigated the effect of ultrasonic vibration on the FSW of pure copper and aluminum alloy. Their study observed a lower thickness of the IMC layer with UVeFSW resulted in a joint with higher tensile strength in comparison to FSW. Ambekar et al. [157] optimized welding parameters for joint tensile strength and microhardness while FSW of AA2024-T4 aluminum alloy. Their study observed better optimization results with ANN-PSO (Particle Swarm Optimization) integrated approach. Taysom et al. [158] developed the predictive model for temperature distribution during FSW considering the hybrid heat source model and first-order plus dead time (FOPDT) model. Their study found that the hybrid heat source model was having a better control over the temperature.

Chen et al. [159] investigated the effect of threaded pin geometry on material flow during FSW of Al-Mg-Zn alloy using the CFD technique. Their study observed that the threaded pin was very crucial in developing vertical pressure gradient and hence, the proper

material flow from top to bottom. Moreover, the threaded pin also improved the material flow velocity and strain rate.

Sabari et al. [160] tried to evaluate mechanical properties and microstructural characteristics of AA2519-T87 aluminum alloy joints made by FSW and underwater FSW (UWFSW). Their study observed higher tensile strength and higher joint efficiency with UWFSW in comparison to conventional FSW. They also estimated the temperature distribution and width of TMAZ by developing an FEA model. Kim et al. [161] developed the FEM model to predict the hardness of the FSW joints of AA6061. FE simulation was performed using the quench factor analysis and bonding criterion.

Zhang et al. [162] investigated the heat flux distribution during FSW of AA2024-T4 using CFD. Their study observed the maximum plastic deformation at the inner part of the shoulder whereas maximum heat flux in the periphery of the shoulder. They also observed a sliding and sticking state at the tool and workpiece interface. Rzaev et al. [163] developed a mathematical model to predict temperature dynamics considering the effect of temperature distribution and input power. The developed model can be useful for the measurement of liner velocity in FSW. Sudhagar et al. [164] optimized tool offset, tool rotational speed, and welding speed for maximizing hardness, impact strength, and tensile strength of welded joint during FSW of aluminum 2024 alloy.

From the literature reviewed it is seen that sufficient attempts were made by researchers on parametric optimization and modeling of the FSW process. However, most of the optimization studies were carried out using traditional methods of optimization. Although modeling attempts in FSW are reported, most of the efforts have been made to model temperature distribution in FSW. This literature review finds ample scope for multi-objective optimization of the FSW process using non-traditional (advanced optimization methods) methods of optimization such as non-sorted genetic algorithm-II (NSGA-II), simulated annealing (SA), particle swarm optimization techniques (PSO), and fuzzy inference systems.

With a view to understanding parametric effects on FSW performances, this study finds the

necessity to develop predictive models for mechanical properties such as fatigue strength, residual stress, tensile strength, grain refinement, and corrosion resistance. Attempts have been made by the researchers to understand the microstructural and metallurgical evolution and their effect on mechanical properties of welded joints of similar and dissimilar aluminum alloys [165-167]. However, a comprehensive understanding of the microstructural refinement, metallurgical features, and effect of post-weld treatments on mechanical properties during FSW and hybrid-FSW of similar and dissimilar high strength aluminum alloy joints need to be investigated. Also, this study finds few studies on the mechanical behavior of high strength AA7075 FSW joints considering the effect of process parameters and hybrid-FSW techniques. Attempts have been made by the researchers on parametric optimization and modeling of the FSW process. However, almost no studies reported the process optimization of FSW of AA7075 alloys. Moreover, most of the efforts have been made to model temperature distribution in FSW. Very few studies developed mathematical models to predict UTS, microhardness and surface roughness.

## 8. Conclusions

This study presents state of the art in friction stir welding (FSW) of similar and dissimilar aluminum alloys to give proper attention to the various researcher works. A comprehensive literature review on FSW and hybrid ultrasonic vibration-assisted (UVEFSW) is presented to understand the applicability of the process for difficult-to-join materials and to get a joint with better mechanical properties. Researchers' works on FSW/hybrid-FSW considering different tool materials and geometries are also presented as the selection of the tool geometry is very crucial and plays an important role in obtaining quality joint. Further, researchers' works that were attempted to evaluate the welding performance are presented to understand the effect of FSW process parameters, joining technique, and post-weld treatments on the mechanical properties of welded joints. This study also presents attempts made by researchers to model and optimize FSW

performance to having more understanding of parametric effect during FSW of aluminum alloys. In the following the summary of the researchers' works with an emphasize on further investigations needed while joining aluminum alloys is mentioned:

- Ultrasonic vibration-assisted friction stir welding (UVEFSW); hybrid-FSW produced welded joint with better mechanical properties in comparison to joint properties obtained with conventional FSW and fusion welding techniques. However, further studies are required to comparatively evaluate FSW performance with the application of ultrasonic frequency combinedly or individually on advancing and retreating sides of plates.
- It is seen that tools with a flat shoulder and circular pin profiles were most commonly used to join similar and dissimilar aluminum alloys. However, further investigations are required to obtain optimum pin profile and shoulder shape for better mechanical properties of welded joints. It is seen that a conical threaded tool with a flat shoulder produced better quality joint in comparison to square and triangular pin profile tools. However, very few attempts were reported on the use of hybrid tools during FSW of aluminum alloys.
- It has been observed that FSW process parameters and joining technique (conventional or hybrid) significantly affected joint tensile strength, fatigue strength, microhardness, microstructure, corrosion resistance, and residual stresses. It is seen that FSW performed with water as a cooling medium lowered heat affected zone and produced ultrafine grain structure resulting in improved tensile strength, microhardness, and joint efficiency.
- It is reported that the presence of SiC nanoparticles in the microstructure increased the fatigue life of the component. Further, HAZ adjacent to the nugget zone were observed to be more susceptible to corrosion. Higher residual stresses were observed on the advancing side and its distribution was asymmetric in nature. Residual stresses in the welded joint were observed to be prominently affected by tool

rotation and negligibly with welding speed (tool traverse). It is seen that the finer the grain size, the higher the tensile strength and fatigue strength. However, more studies are required to obtain corrosion resistance of welded joint considering the effect of FSW process parameters and hybrid-FSW techniques.

- Mostly shot peening and laser shock peening treatments are prominently reported in the literature as post-weld treatments to obtain better joint efficiency and joint strength. Laser shock peening treated welded joints resulted in finer grain size, better corrosion resistance, and higher fatigue strength.
- Optimization of FSW mostly attempted using traditional methods of optimization. And, most of the modeling attempts were made to obtain temperature distribution during FSW. However, multi-objective optimization of FSW needs to be undertaken using advanced optimization methods such as non-sorted genetic algorithm-II (NSGA-II), simulated annealing (SA), particle swarm optimization techniques (PSO), and fuzzy inference systems.

## References

- [1] R. Kumar, R. Singh, I. P. S. Ahuja, R. Penna and L. Feo, "Weldability of thermoplastic materials for friction stir welding- A state of art review and future applications," *Compos. Part B Eng.*, Vol. 137, No. 1, pp. 1–15, (2018).
- [2] S. J. Doshi, A. V Gohil, N. Mehta and S. Vaghasiya, "Challenges in Fusion Welding of Al alloy for Body in White," *Mater. Today Proc.*, Vol. 5, No. 2, pp. 6370–6375, (2018).
- [3] P. M. G. P. Moreira, M. A. V. De Figueiredo and P. M. S. T. de Castro, "Fatigue behaviour of FSW and MIG weldments for two aluminium alloys," *Theor. Appl. Fract. Mech.*, Vol. 48, No. 2, pp. 169–177, (2007).
- [4] B. Sadeghian, A. Taherizadeh and M. Atapour, "Simulation of weld morphology during friction stir welding of aluminum- stainless steel joint," *J. Mater.*



- Process. Technol.*, Vol. 259, No. 1, pp. 96–108, (2018).
- [5] G. L. Qin, Y. H. Su and S. J. Wang, “Microstructures and properties of welded joint of aluminum alloy to galvanized steel by Nd:YAG laser + MIG arc hybrid brazing-fusion welding,” *Trans. Nonferrous Met. Soc. China (English Ed.)*, Vol. 24, No. 4, pp. 989–995, (2014).
- [6] F. Nie *et al.*, “Microstructure and Mechanical Properties of Pulse MIG Welded 6061/A356 Aluminum Alloy Dissimilar Butt Joints,” *J. Mater. Sci. Technol.*, Vol. 34, No. 3, pp. 551–560, (2018).
- [7] Q. Chen, S. Lin, C. Yang, C. Fan and H. Ge, “Grain fragmentation in ultrasonic-assisted TIG weld of pure aluminum,” *Ultrason. Sonochem.*, Vol. 39, No. 1, pp. 403–413, (2017).
- [8] L. J. Zhang *et al.*, “A comparative study on the microstructure and properties of copper joint between MIG welding and laser-MIG hybrid welding,” *Mater. Des.*, Vol. 110, No. 1, pp. 35–50, (2016).
- [9] H. K. Lee, K. S. Chun, S. H. Park and C. Y. Kang, “Control of surface defects on plasma-MIG hybrid welds in cryogenic aluminum alloys,” *Int. J. Nav. Archit. Ocean Eng.*, Vol. 7, No. 4, pp. 770–783, (2015).
- [10] A. Fritzsche, K. Hilgenberg, F. Teichmann, H. Pries, K. Dilger and M. Rethmeier, “Improved degassing in laser beam welding of aluminum die casting by an electromagnetic field,” *J. Mater. Process. Technol.*, Vol. 253, No. 1, pp. 51–56, (2018).
- [11] Y. Zhang, X. Song, L. Chang and S. Wu, “Fatigue Lifetime of Laser-MIG Hybrid Welded Joint of 7075-T6 Aluminum Alloy by in-situ Observation,” *Xiyou Jinshu Cailiao Yu Gongcheng/Rare Met. Mater. Eng.*, Vol. 46, No. 9, pp. 2411–2416, (2017).
- [12] Y. Wang, B. Qi, B. Cong, M. Zhu and S. Lin, “Keyhole welding of AA2219 aluminum alloy with double-pulsed variable polarity gas tungsten arc welding,” *J. Manuf. Process.*, Vol. 34(A), No. 1, pp. 179–186, (2018).
- [13] D. Cai, S. Han, S. Zheng, Z. Luo, Y. Zhang and K. Wang, “Microstructure and corrosion resistance of Al5083 alloy hybrid plasma-MIG welds,” *J. Mater. Process. Technol.*, Vol. 255, No. 1, pp. 530–535, (2018).
- [14] H. Li, J. Zou, J. Yao and H. Peng, “The effect of TIG welding techniques on microstructure, properties and porosity of the welded joint of 2219 aluminum alloy,” *J. Alloys Compd.*, Vol. 727, No. 1, pp. 531–539, (2017).
- [15] Y. Bai, H. M. Gao, L. Wu, Z. H. Ma and N. Cao, “Influence of plasma-MIG welding parameters on aluminum weld porosity by orthogonal test,” *Trans. Nonferrous Met. Soc. China (English Ed.)*, Vol. 20, No. 8, pp. 1392–1396, (2010).
- [16] F. Li, W. Tao, G. Peng, J. Qu and L. Li, “Behavior and stability of droplet transfer under laser-MIG hybrid welding with synchronized pulse modulations,” *J. Manuf. Process.*, Vol. 54, No. 1, pp. 70–79, (2020).
- [17] I. Bunaziv, O. M. Akselsen, A. Salminen and A. Unt, “Fiber laser-MIG hybrid welding of 5 mm 5083 aluminum alloy,” *J. Mater. Process. Technol.*, Vol. 233, No. 1, pp. 107–114, (2016).
- [18] X. Zhan, D. Zhang, Y. Wei and Y. Wang, “Research on the microstructure and properties of laser-MIG hybrid welded joint of Invar alloy,” *Opt. Laser Technol.*, Vol. 97, No. 1, pp. 124–136, (2017).
- [19] Y. Bai, H. M. Gao and L. Qiu, “Droplet transition for plasma-MIG welding on aluminium alloys,” *Trans. Nonferrous Met. Soc. China (English Ed.)*, Vol. 20, No. 12, pp. 2234–2239, (2010).
- [20] Z. Ye *et al.*, “Combined effects of MIG and TIG arcs on weld appearance and interface properties in Al/steel double-sided butt welding-brazing,” *J. Mater. Process. Technol.*, Vol. 250, No. 1, pp. 25–34, (2017).
- [21] Y. Peng, C. Shen, Y. Zhao and Y. Chen, “Comparison of Electrochemical Behaviors between FSW and MIG Joints for 6082 Aluminum Alloy,” *Xiyou Jinshu Cailiao Yu Gongcheng/Rare Met. Mater. Eng.*, Vol. 46, No. 2, pp. 344–348, (2017).

- [22] G. Qin, Y. Ji, H. Ma and Z. Ao, "Effect of modified flux on MIG arc brazing-fusion welding of aluminum alloy to steel butt joint," *J. Mater. Process. Technol.*, Vol. 245, No. 1, pp. 115–121, (2017).
- [23] Y. Miao, Z. Ma, X. Yang, J. Liu and D. Han, "Experimental study on microstructure and mechanical properties of AA6061/Ti-6Al-4V joints made by bypass-current MIG welding-brazing," *J. Mater. Process. Technol.*, Vol. 260, No. 1, pp. 104–111, (2018).
- [24] S. Sudhagar, M. Sakthivel and P. Ganeshkumar, "Monitoring of friction stir welding based on vision system coupled with Machine learning algorithm," *Measurement*, Vol. 144, No. 1, pp.135–143, (2019).
- [25] J. D. M. Costa, J. S. Jesus, A. Loureiro, J. A. M. Ferreira and L. P. Borrego, "Fatigue life improvement of mig welded aluminium T-joints by friction stir processing," *Int. J. Fatigue*, Vol. 61, No. 1, pp. 244–254, (2014).
- [26] Z. Ye *et al.*, "Microstructure and mechanical properties of 5052 aluminum alloy/mild steel butt joint achieved by MIG-TIG double-sided arc welding-brazing," *Mater. Des.*, Vol. 123, No. 1, pp. 69–79, (2017).
- [27] S. Sinhmar and D. K. Dwivedi, "A study on corrosion behavior of friction stir welded and tungsten inert gas welded AA2014 aluminium alloy," *Corros. Sci.*, Vol. 133, No. 1, pp. 25–35, (2018).
- [28] S. R. Mokabberi, M. Movahedi and A. H. Kokabi, "Effect of interlayers on softening of aluminum friction stir welds," *Mater. Sci. Eng. A*, Vol. 727, No. 1, pp. 1–10, (2018).
- [29] M. Ericsson and R. Sandström, "Influence of welding speed on the fatigue of friction stir welds, and comparison with MIG and TIG," *Int. J. Fatigue*, Vol. 25, No. 12, pp. 1379–1387, (2003).
- [30] A. Squillace, A. De Fenzo, G. Giorleo and F. Bellucci, "A comparison between FSW and TIG welding techniques: Modifications of microstructure and pitting corrosion resistance in AA 2024-T3 butt joints," *J. Mater. Process. Technol.*, Vol. 152, No. 1, pp. 97–105, (2004).
- [31] V. Fahimpour, S. K. Sadrnezhad and F. Karimzadeh, "Corrosion behavior of aluminum 6061 alloy joined by friction stir welding and gas tungsten arc welding methods," *Mater. Des.*, Vol. 39, No. 1, pp. 329–333, (2012).
- [32] A. Yazdipour and A. Heidarzadeh, "Effect of friction stir welding on microstructure and mechanical properties of dissimilar Al 5083-H321 and 316L stainless steel alloy joints," *J. Alloys Compd.*, Vol. 680, No. 1, pp. 595–603, (2016).
- [33] J. T. Xiong, J. L. Li, J. W. Qian, F. S. Zhang and W. D. Huang, "High strength lap joint of aluminium and stainless steels fabricated by friction stir welding with cutting pin," *Sci. Technol. Weld. Join.*, Vol. 17, No. 3, pp. 196–201, (2012).
- [34] Y. Zhang, J. Huang, Z. Ye and Z. Cheng, "An investigation on butt joints of Ti6Al4V and 5A06 using MIG/TIG double-side arc welding-brazing," *J. Manuf. Process.*, Vol. 27, No. 1, pp. 221–225, (2017).
- [35] G. H. S. F. L. Carvalho, I. Galvão, R. Mendes, R. M. Leal and A. Loureiro, "Explosive welding of aluminium to stainless steel," *J. Mater. Process. Technol.*, Vol. 262, No. 1, pp. 340–349, (2018).
- [36] D. Löveborn, J. K. Larsson and K. A. Persson, "Weldability of Aluminium Alloys for Automotive Applications," *Phys. Procedia*, Vol. 89, No. 1, pp. 89–99, (2017).
- [37] P. Liu, S. Sun, S. Xu, Y. Li and G. Ren, "Microstructure and properties in the weld surface of friction stir welded 7050-T7451 aluminium alloys by laser shock peening," *Vacuum*, Vol. 152, No. 1, pp. 25–29, (2018).
- [38] L. Shi, C. S. Wu and X. C. Liu, "Modeling the effects of ultrasonic vibration on friction stir welding," *J. Mater. Process. Technol.*, Vol. 222, No. 1, pp. 91–102, (2015).
- [39] X. C. Liu and C. S. Wu, "Experimental study on ultrasonic vibration enhanced

- friction stir welding,” *Proc. 1st Int. Jt. Symp. Join. Weld.*, pp. 151–154, (2013).
- [40] C. Xu, G. Sheng, X. Cao and X. Yuan, “Evolution of Microstructure, Mechanical Properties and Corrosion Resistance of Ultrasonic Assisted Welded-Brazed Mg/Ti Joint,” *J. Mater. Sci. Technol.*, Vol. 32, No. 12, pp. 1253–1259, (2016).
- [41] X. Liu, C. Wu and G. K. Padhy, “Characterization of plastic deformation and material flow in ultrasonic vibration enhanced friction stir welding,” *Scr. Mater.*, Vol. 102, No. 1, pp. 95–98, (2015).
- [42] M. Shakil, N. H. Tariq, M. Ahmad, M. A. Choudhary, J. I. Akhter and S. S. Babu, “Effect of ultrasonic welding parameters on microstructure and mechanical properties of dissimilar joints,” *Mater. Des.*, Vol. 55, No. 1, pp. 263–273, (2014).
- [43] Z. Lei, J. Bi, P. Li, T. Guo, Y. Zhao and D. Zhang, “Analysis on welding characteristics of ultrasonic assisted laser welding of AZ31B magnesium alloy,” *Opt. Laser Technol.*, Vol. 105, No. 1, pp. 15–22, (2018).
- [44] S. Kumar, C. S. Wu, G. K. Padhy and W. Ding, “Application of ultrasonic vibrations in welding and metal processing: A status review,” *J. Manuf. Process.*, Vol. 26, No. 1, pp. 295–322, (2017).
- [45] M. Wu, C. S. Wu and S. Gao, “Effect of ultrasonic vibration on fatigue performance of AA 2024-T3 friction stir weld joints,” *J. Manuf. Process.*, Vol. 29, No. 1, pp. 85–95, (2017).
- [46] Y. B. Zhong, C. S. Wu and G. K. Padhy, “Effect of ultrasonic vibration on welding load, temperature and material flow in friction stir welding,” *J. Mater. Process. Technol.*, Vol. 239, No. 1, pp. 273–283, (2017).
- [47] X. C. Liu and C. S. Wu, “Elimination of tunnel defect in ultrasonic vibration enhanced friction stir welding,” *Mater. Des.*, Vol. 90, No. 1, pp. 350–358, (2016).
- [48] S. Gao, C. S. Wu, G. K. Padhy and L. Shi, “Evaluation of local strain distribution in ultrasonic enhanced Al 6061-T6 friction stir weld nugget by EBSD analysis,” *Mater. Des.*, Vol. 99, No. 1, pp. 135–144, (2016).
- [49] Z. Liu, X. Meng, S. Ji, Z. Li and L. Wang, “Improving tensile properties of Al/Mg joint by smashing intermetallic compounds via ultrasonic-assisted stationary shoulder friction stir welding,” *J. Manuf. Process.*, Vol. 31, No. 1, pp. 552–559, (2018).
- [50] X. Meng, Y. Jin, S. Ji and D. Yan, “Improving friction stir weldability of Al/Mg alloys via ultrasonically diminishing pin adhesion,” *J. Mater. Sci. Technol.*, Vol. 34, No. 10, pp. 1817–1822, (2018).
- [51] G. K. Padhy, C. S. Wu, S. Gao and L. Shi, “Local microstructure evolution in Al 6061-T6 friction stir weld nugget enhanced by ultrasonic vibration,” *Mater. Des.*, Vol. 92, No. 1, pp. 710–723, (2016).
- [52] X. C. Liu and C. S. Wu, “Material flow in ultrasonic vibration enhanced friction stir welding,” *J. Mater. Process. Technol.*, Vol. 225, No. 1, pp. 32–44, (2015).
- [53] S. Gao, C. S. Wu and G. K. Padhy, “Material flow, microstructure and mechanical properties of friction stir welded AA 2024-T3 enhanced by ultrasonic vibrations,” *J. Manuf. Process.*, Vol. 30, No. 1, pp. 385–395, (2017).
- [54] G. K. Padhy, C. S. Wu and S. Gao, “Subgrain formation in ultrasonic enhanced friction stir welding of aluminium alloy,” *Mater. Lett.*, Vol. 183, No. 1, pp. 34–39, (2016).
- [55] S. Ji, X. Meng, Z. Liu, R. Huang and Z. Li, “Dissimilar friction stir welding of 6061 aluminum alloy and AZ31 magnesium alloy assisted with ultrasonic,” *Mater. Lett.*, Vol. 201, pp. No. 1, 173–176, (2017).
- [56] X. Q. Lv, C. S. Wu and G. K. Padhy, “Diminishing intermetallic compound layer in ultrasonic vibration enhanced friction stir welding of aluminum alloy to magnesium alloy,” *Mater. Lett.*, Vol. 203, No. 1, pp. 81–84, (2017).
- [57] K. P. Mehta and V. J. Badheka, “Hybrid approaches of assisted heating and cooling for friction stir welding of copper to aluminum joints,” *J. Mater. Process.*

- Technol.*, Vol. 239, No. 1, pp. 336–345, (2017).
- [58] L. Shi, C. S. Wu, G. K. Padhy and S. Gao, “Numerical simulation of ultrasonic field and its acoustoplastic influence on friction stir welding,” *Mater. Des.*, Vol. 104, No. 1, pp. 102–115, (2016).
- [59] S. Kumar, “Ultrasonic assisted friction stir processing of 6063 aluminum alloy,” *Arch. Civ. Mech. Eng.*, Vol. 16, No. 3, pp. 473–484, (2016).
- [60] M. Thomä, G. Wagner, B. Straß, B. Wolter, S. Benfer and W. Fürbeth, “Ultrasound enhanced friction stir welding of aluminum and steel: Process and properties of EN AW 6061/DC04-Joints,” *J. Mater. Sci. Technol.*, Vol. 34, No. 1, pp. 163–172, (2018).
- [61] X. Lv, C. S. Wu, C. Yang and G. K. Padhy, “Weld microstructure and mechanical properties in ultrasonic enhanced friction stir welding of Al alloy to Mg alloy,” *J. Mater. Process. Technol.*, Vol. 254, No. 1, pp. 145–157, (2018).
- [62] P. Mastanaiah, A. Sharma and G. M. Reddy, “Role of hybrid tool pin profile on enhancing welding speed and mechanical properties of AA2219-T6 friction stir welds,” *J. Mater. Process. Technol.*, Vol. 257, No. 1, pp. 257–269, (2018).
- [63] R. Rai, A. De, H. K. D. H. Bhadeshia and T. DebRoy, “Review: Friction stir welding tools,” *Sci. Technol. Weld. Join.*, Vol. 16, No. 4, pp. 325–342, (2011).
- [64] W. Hou, Y. Shen, G. Huang, Y. Yan, C. Guo and J. Li, “Dissimilar friction stir welding of aluminum alloys adopting a novel dual-pin tool: Microstructure evolution and mechanical properties,” *J. Manuf. Process.*, Vol. 36, No. 1, pp. 613–620, (2018).
- [65] S. Zhao *et al.*, “Effects of tool geometry on friction stir welding of AA6061 to TRIP steel,” *J. Mater. Process. Technol.*, Vol. 261, No. 1, pp. 39–49, (2018).
- [66] R. Beygi, M. Z. Mehrizi, D. Verdera and A. Loureiro, “Influence of tool geometry on material flow and mechanical properties of friction stir welded Al-Cu bimetal,” *J. Mater. Process. Technol.*, Vol. 255, No. 1, pp. 739–748, (2018).
- [67] M. Rezaee Hajideh, M. Farahani, S. A. D. Alavi and N. Molla Ramezani, “Investigation on the effects of tool geometry on the microstructure and the mechanical properties of dissimilar friction stir welded polyethylene and polypropylene sheets,” *J. Manuf. Process.*, Vol. 26, No. 1, pp. 269–279, (2017).
- [68] G. Chen, G. Wang, Q. Shi, Y. Zhao, Y. Hao and S. Zhang, “Three-dimensional thermal-mechanical analysis of retractable pin tool friction stir welding process,” *J. Manuf. Process.*, Vol. 41, No. 1, pp. 1–9, (2019).
- [69] J. M. Piccini and H. G. Svoboda, “Tool geometry optimization in friction stir spot welding of Al-steel joints,” *J. Manuf. Process.*, vol. 26, No. 1, pp. 142–154, (2017).
- [70] K. Kumar, S. V. Kailas and T. S. Srivatsan, “Influence of tool geometry in friction stir welding,” *Mater. Manuf. Process.*, Vol. 23, No. 2, pp. 188–194, (2008).
- [71] A. Garg and A. Bhattacharya, “Strength and failure analysis of similar and dissimilar friction stir spot welds: Influence of different tools and pin geometries,” *Mater. Des.*, Vol. 127, No. 1, pp. 272–286, (2017).
- [72] K. Ullegaddi, V. Murthy, R. N. Harsha and Manjunatha, “Friction Stir Welding Tool Design and Their Effect on Welding of AA-6082 T6,” *Mater. Today Proc.*, Vol. 4, No. 8, pp. 7962–7970, (2017).
- [73] O. Lorrain, V. Favier, H. Zahrouni and D. Lawrjaniec, “Understanding the material flow path of friction stir welding process using unthreaded tools,” *J. Mater. Process. Technol.*, Vol. 210, No. 4, pp. 603–609, (2010).
- [74] H. Badarinarayan, Y. Shi, X. Li and K. Okamoto, “Effect of tool geometry on hook formation and static strength of friction stir spot welded aluminum 5754-O sheets,” *Int. J. Mach. Tools Manuf.*, Vol. 49, No. 11, pp. 814–823, (2009).
- [75] D. Bakavos and P. B. Prangnell, “Effect of reduced or zero pin length and anvil insulation on friction stir spot welding thin

- gauge 6111 automotive sheet,” *Sci. Technol. Weld. Join.*, Vol. 14, No. 5, pp. 443–456, (2009).
- [76] A. Suri, “An Improved FSW Tool for Joining Commercial Aluminum Plates,” *Procedia Mater. Sci.*, Vol. 6, No. 1, pp. 1857–1864, (2014).
- [77] K. P. Yuvaraj, P. Ashoka Varthanan, L. Haribabu, R. Madhubalan and K. P. Boopathiraja, “Optimization of FSW tool parameters for joining dissimilar AA7075-T651 and AA6061 aluminium alloys using Taguchi Technique,” *Mater. Today Proc.*, (2020).
- [78] V. Murthy, U. Kalmeshwar, B. M. Rajaprakash and R. Rajashekar, “Study on influence of concave geometry shoulder tool in Friction Stir Welding (FSW) by using Image Processing and Acoustic Emission Techniques,” *Mater. Today Proc.*, Vol. 5, No. 13, pp. 27004–27017, (2018).
- [79] K. Krasnowski, C. Hamilton and S. Dymek, “Influence of the tool shape and weld configuration on microstructure and mechanical properties of the Al 6082 alloy FSW joints,” *Arch. Civ. Mech. Eng.*, Vol. 15, No. 1, pp. 133–141, (2015).
- [80] J. John, S. P. Shanmughanatan and M. B. Kiran, “Effect of tool geometry on microstructure and mechanical Properties of friction stir processed AA2024-T351 aluminium alloy,” *Mater. Today Proc.*, Vol. 5, No. 1, pp. 2965–2979, (2018).
- [81] A. Paul, S. Kumar Sinha, P. P. Chattopadhyay and S. Ganguly, “Anomalous enhancement of strength-ductility combination in FSW joints of AA7039,” *Manuf. Lett.*, Vol. 22, No. 1, pp. 1–5, (2019).
- [82] M. S. Srinivasa Rao, B. V. R. Ravi Kumar and M. Manzoor Hussain, “Experimental study on the effect of welding parameters and tool pin profiles on the IS:65032 aluminum alloy FSW joints,” *Mater. Today Proc.*, Vol. 4, No. 2, pp. 1394–1404, (2017).
- [83] C. S. Jawalkar and S. Kant, “A Review on use of Aluminium Alloys in Aircraft Components,” *i-manager’s J. Mater. Sci.*, Vol. 3, No. 3, pp. 33–38, (2015).
- [84] V. V. K. Prasad Rambabu, N. Esvara Prasad and R. J. H. Wanhill, “Aerospace Materials and Material Technologies”, *Aerospace Materials*, Vol. 1, pp. 29-52, (2017).
- [85] J. A. Hamed, “Effect of welding heat input and post-weld aging time on microstructure and mechanical properties in dissimilar friction stir welded AA7075–AA5086,” *Trans. Nonferrous Met. Soc. China (English Ed.)*, Vol. 27, No. 8, pp. 1707–1715, (2017).
- [86] D. Rao, K. Huber, J. Heerens, J. F. dos Santos and N. Huber, “Asymmetric mechanical properties and tensile behaviour prediction of aluminium alloy 5083 friction stir welding joints,” *Mater. Sci. Eng. A*, Vol. 565, No. 1, pp. 44–50, (2013).
- [87] S. Sree Sabari, S. Malarvizhi, V. Balasubramanian and G. Madusudhan Reddy, “Experimental and numerical investigation on under-water friction stir welding of armour grade AA2519-T87 aluminium alloy,” *Def. Technol.*, Vol. 12, No. 4, pp. 324–333, (2016).
- [88] Y. Huang, X. Meng, Y. Zhang, J. Cao, and J. Feng, “Micro friction stir welding of ultra-thin Al-6061 sheets,” *J. Mater. Process. Technol.*, Vol. 250, No. 1, pp. 313–319, (2017).
- [89] J. Fathi, P. Ebrahimzadeh, R. Farasati and R. Teimouri, “Friction stir welding of aluminum 6061-T6 in presence of watercooling: Analyzing mechanical properties and residual stress distribution,” *Int. J. Light. Mater. Manuf.*, Vol. 2, No. 2, pp. 107–115, (2019).
- [90] M. Bahrami, N. Helmi, K. Dehghani and M. K. B. Givi, “Exploring the effects of SiC reinforcement incorporation on mechanical properties of friction stir welded 7075 aluminum alloy: Fatigue life, impact energy, tensile strength,” *Mater. Sci. Eng. A*, Vol. 595, No. 1, pp. 173–178, (2014).
- [91] D. Ghahremani and K. Farhangdoost, “Influence of welding parameters on fracture toughness and fatigue crack growth rate in friction stir welded nugget of 2024-T351 aluminum alloy joints,”

- Trans. Nonferrous Met. Soc. China (English Ed.)*, Vol. 26, No. 10, pp. 2567–2585, (2016).
- [92] Z. Liu, H. Zhang, H. Feng, Z. Yan and P. Dong, “Effects of surface gradient nanostructuring on the fatigue behavior of the friction stir welded AlZnMgCu alloy,” *Mater. Lett.*, Vol. 252, No. 1, pp. 329–332, (2019).
- [93] R. I. Rodriguez, J. B. Jordon, P. G. Allison, T. Rushing and L. Garcia, “Low-cycle fatigue of dissimilar friction stir welded aluminum alloys,” *Mater. Sci. Eng. A*, Vol. 654, No. 1, pp. 236–248, (2016).
- [94] I. Vysotskiy, S. Malopheyev, S. Rahimi, S. Mironov and R. Kaibyshev, “Unusual fatigue behavior of friction-stir welded Al–Mg–Si alloy,” *Mater. Sci. Eng. A*, Vol. 760, No. 1, pp. 277–286, (2019).
- [95] S. Guo, L. Shah, R. Ranjan, S. Walbridge, and A. Gerlich, “Effect of quality control parameter variations on the fatigue performance of aluminum friction stir welded joints,” *Int. J. Fatigue*, Vol. 118, No. 1, pp. 150–161, (2019).
- [96] P. Cavaliere and F. Panella, “Effect of tool position on the fatigue properties of dissimilar 2024-7075 sheets joined by friction stir welding,” *J. Mater. Process. Technol.*, Vol. 206, No. 1–3, pp. 249–255, (2008).
- [97] C. Yang et al., “High-cycle fatigue and fracture behavior of double-side friction stir welded 6082Al ultra-thick plates,” *Eng. Fract. Mech.*, Vol. 226, No. 106887, (2020).
- [98] S. Kumar, A. K. Srivastava, R. K. Singh and S. P. Dwivedi, “Experimental study on hardness and fatigue behavior in joining of AA5083 and AA6063 by friction stir welding,” *Mater. Today Proc.*, Vol. 25, No. 4, pp. 646–648, (2019).
- [99] C. Deng, R. Gao, B. Gong, T. Yin and Y. Liu, “Correlation between micro-mechanical property and very high cycle fatigue (VHCF) crack initiation in friction stir welds of 7050 aluminum alloy,” *Int. J. Fatigue*, Vol. 104, No. 1, pp. 283–292, (2017).
- [100] M. Milčić, Z. Burzić, I. Radisavljević, T. Vuherer, D. Milčić and V. Grabulov, “Experimental investigation of fatigue properties of FSW in AA2024-T351,” *Procedia Struct. Integr.*, Vol. 13, No. 1, pp. 1977–1984, (2018).
- [101] G. M. F. Essa, H. M. Zakria, T. S. Mahmoud and T. A. Khalifa, “Microstructure examination and microhardness of friction stir welded joint of (AA7020-O) after PWHT,” *HBRC J.*, Vol. 14, No. 1, pp. 22–28, (2018).
- [102] O. S. Salih, H. Ou, X. Wei and W. Sun, “Microstructure and mechanical properties of friction stir welded AA6092/SiC metal matrix composite,” *Mater. Sci. Eng. A*, Vol. 742, No. 1, pp. 78–88, (2019).
- [103] J. S. Leon and V. Jayakumar, “Some Investigations on Thermal Analysis of Aluminium Alloys in Friction Stir Welding,” *Am. J. Mech. Eng. Autom.*, Vol. 2, No. 3, pp. 36–39, (2015).
- [104] H. Bisadi, S. Rasaei and M. Farahmand, “Experimental study of the temperature distribution and microstructure of plunge stage in friction stir welding process by the tool with triangle pin,” *Arch. Mech. Eng.*, Vol. 61, No. 3, pp. 483–493, (2014).
- [105] B. B. Wang, F. F. Chen, F. Liu, W. G. Wang, P. Xue and Z. Y. Ma, “Enhanced Mechanical Properties of Friction Stir Welded 5083Al-H19 Joints with Additional Water Cooling,” *J. Mater. Sci. Technol.*, Vol. 33, No. 9, pp. 1009–1014, (2017).
- [106] S. Ma, Y. Zhao, J. Zou, K. Yan and C. Liu, “The effect of laser surface melting on microstructure and corrosion behavior of friction stir welded aluminum alloy 2219,” *Opt. Laser Technol.*, Vol. 96, No. 1, pp. 299–306, (2017).
- [107] P. Avinash, M. Manikandan, N. Arivazhagan, R. K. Devendranath and S. Narayanan, “Friction stir welded butt joints of AA2024 T3 and AA7075 T6 aluminum alloys,” *Procedia Eng.*, Vol. 75, No. 1, pp. 98–102, (2014).
- [108] M. M. Moradi, H. Jamshidi Aval, R. Jamaati, S. Amir Khanlou and S. Ji, “Microstructure and texture evolution of

- friction stir welded dissimilar aluminum alloys: AA2024 and AA6061,” *J. Manuf. Process.*, Vol. 32, No. 1, pp. 1–10, (2018).
- [109] T. Dursun and C. Soutis, “Recent developments in advanced aircraft aluminium alloys,” *Mater. Des.*, Vol. 56, No. 1, pp. 862–871, (2014).
- [110] Y. Chen *et al.*, “Macro-galvanic effect and its influence on corrosion behaviors of friction stir welding joint of 7050-T76 Al alloy,” *Corros. Sci.*, Vol. 164, No. 108360, (2020).
- [111] S. Sinhmar and D. K. Dwivedi, “Investigation of mechanical and corrosion behavior of friction stir weld joint of aluminium alloy,” *Mater. Today Proc.*, Vol. 18, No. 1, pp. 4542–4548, (2019).
- [112] A. Squillace, A. De Fenzo, G. Giorleo and F. Bellucci, “A comparison between FSW and TIG welding techniques: Modifications of microstructure and pitting corrosion resistance in AA 2024-T3 butt joints,” *J. Mater. Process. Technol.*, Vol. 152, No. 1, pp. 97–105, (2004).
- [113] D. Balaji Naik, C. H. Venkata Rao, K. Srinivasa Rao, G. Madhusudan Reddy and G. Rambabu, “Optimization of friction stir welding parameters to improve corrosion resistance and hardness of AA2219 aluminum alloy welds,” *Mater. Today Proc.*, Vol. 15, No. 1, pp. 76–83, (2019).
- [114] S. Maggiolino and C. Schmid, “Corrosion resistance in FSW and in MIG welding techniques of AA6XXX,” *J. Mater. Process. Technol.*, Vol. 197, No. 1–3, pp. 237–240, (2008).
- [115] P. Liu, S. Sun and J. Hu, “Effect of laser shock peening on the microstructure and corrosion resistance in the surface of weld nugget zone and heat-affected zone of FSW joints of 7050 Al alloy,” *Opt. Laser Technol.*, Vol. 112, No. 1, pp. 1–7, (2019).
- [116] S. D. Meshram, A. G. Paradkar, G. M. Reddy and S. Pandey, “Friction stir welding: An alternative to fusion welding for better stress corrosion cracking resistance of maraging steel,” *J. Manuf. Process.*, Vol. 25, No. 1, pp. 94–103, (2017).
- [117] H. Jafarlou, H. Mohammadzadeh Jamalian and M. Tamjidi Eskandar, “Investigation into the role of pin geometry on the corrosion behavior of multi-pass FSWed joints of Al5086 besides applying Al<sub>2</sub>O<sub>3</sub> nanoparticles,” *J. Manuf. Process.*, Vol. 32, No. 1, pp. 425–431, (2018).
- [118] N. D. Nam, L. T. Dai, M. Mathesh, M. Z. Bian and V. T. H. Thu, “Role of friction stir welding - Traveling speed in enhancing the corrosion resistance of aluminum alloy,” *Mater. Chem. Phys.*, Vol. 173, No. 1, pp. 7–11, (2016).
- [119] S. Sinhmar and D. K. Dwivedi, “Enhancement of mechanical properties and corrosion resistance of friction stir welded joint of AA2014 using water cooling,” *Mater. Sci. Eng. A*, Vol. 684, No. 1, pp. 413–422, (2017).
- [120] S. Sinhmar and D. K. Dwivedi, “A study on corrosion behavior of friction stir welded and tungsten inert gas welded AA2014 aluminium alloy,” *Corros. Sci.*, Vol. 133, No. 1, pp. 25–35, (2018).
- [121] G. D’Urso, C. Giardini, S. Lorenzi, M. Cabrini and T. Pastore, “The influence of process parameters on mechanical properties and corrosion behaviour of friction stir welded aluminum joints,” *Procedia Eng.*, Vol. 207, No. 1, pp. 591–596, (2017).
- [122] Y. Peng, C. Shen, Y. Zhao and Y. Chen, “Comparison of Electrochemical Behaviors between FSW and MIG Joints for 6082 Aluminum Alloy,” *Xiyou Jinshu Cailiao Yu Gongcheng/Rare Met. Mater. Eng.*, Vol. 46, No. 2, pp. 344–348, (2017).
- [123] N. S. M. Nasir, M. K. A. A. Razab, S. Mamat and M. I. Ahmad, “Review on Welding Residual Stress,” *ARPN J. Eng. Appl. Sci.*, Vol. 11, No. 9, pp. 6166–6175, 2016.
- [124] L. Fratini and B. Zuccarello, “An analysis of through-thickness residual stresses in aluminium FSW butt joints,” *Int. J. Mach. Tools Manuf.*, Vol. 46, No. 6, pp. 611–619, (2006).

- [125] T. Sun, M. J. Roy, D. Strong, P. J. Withers and P. B. Prangnell, "Comparison of residual stress distributions in conventional and stationary shoulder high-strength aluminum alloy friction stir welds," *J. Mater. Process. Technol.*, Vol. 242, No. 1, pp. 92–100, (2017).
- [126] J. Schwinn and M. Besel, "Determination of residual stresses in tailored welded blanks with thickness transition for crack assessment," *Eng. Fract. Mech.*, Vol. 208, No. 1, pp. 209–220, (2019).
- [127] Y. Zhan, Y. Li, E. Zhang, Y. Ge and C. Liu, "Laser ultrasonic technology for residual stress measurement of 7075 aluminum alloy friction stir welding," *Appl. Acoust.*, Vol. 145, No.1, pp. 52–59, (2019).
- [128] S. El Mouhri, H. Essoussi, S. Ettaqi and S. Benayoun, "Relationship between Microstructure, Residual Stress and Thermal Aspect in Friction Stir Welding of Aluminum AA1050," *Procedia Manuf.*, Vol. 32, No.1, pp. 889–894, (2019).
- [129] V. Richter-Trummer, E. Suzano, M. Beltrão, A. Roos, J. F. Dos Santos and P. M. S. T. de Castro, "Influence of the FSW clamping force on the final distortion and residual stress field," *Mater. Sci. Eng. A*, Vol. 538, No. 1, pp. 81–88, (2012).
- [130] T. Sun, A. P. Reynolds, M. J. Roy, P. J. Withers and P. B. Prangnell, "The effect of shoulder coupling on the residual stress and hardness distribution in AA7050 friction stir butt welds," *Mater. Sci. Eng. A*, Vol. 735, No. 1, pp. 218–227, (2018).
- [131] L. Buglioni, L. N. Tufaro and H. G. Svoboda, "Thermal Cycles and Residual Stresses in FSW of Aluminum Alloys: Experimental Measurements and Numerical Models," *Procedia Mater. Sci.*, Vol. 9, No. 1, pp. 87–96, (2015).
- [132] M. O. H. Amuda and S. Mridha, "Comparative evaluation of grain refinement in AISI 430 FSS welds by elemental metal powder addition and cryogenic cooling," *Mater. Des.*, Vol. 35, No. 1, pp. 609–618, (2012).
- [133] O. Hatamleh, M. Hill, S. Forth and D. Garcia, "Fatigue crack growth performance of peened friction stir welded 2195 aluminum alloy joints at elevated and cryogenic temperatures," *Mater. Sci. Eng. A*, Vol. 519, No. 1–2, pp. 61–69, (2009).
- [134] O. Hatamleh, R. S. Mishra and O. Oliveras, "Peening effects on mechanical properties in friction stir welded AA 2195 at elevated and cryogenic temperatures," *Mater. Des.*, Vol. 30, No. 8, pp. 3165–3173, (2009).
- [135] M. S. Khorrami, M. Kazeminezhad, Y. Miyashita, N. Saito and A. H. Kokabi, "Influence of ambient and cryogenic temperature on friction stir processing of severely deformed aluminum with SiC nanoparticles," *J. Alloys Compd.*, Vol. 718, No. 1, pp. 361–372, (2017).
- [136] M. S. Khorrami, M. Kazeminezhad, Y. Miyashita, N. Saito and A. H. Kokabi, "Influence of ambient and cryogenic temperature on friction stir processing of severely deformed aluminum with SiC nanoparticles," *J. Alloys Compd.*, Vol. 718, No. 1, pp. 361–372, (2017).
- [137] S. Singh and G. Dhuria, "Investigation of post weld cryogenic treatment on weld strength in friction stir welded dissimilar aluminium alloys AA2014-T651 and AA7075-T651," *Mater. Today Proc.*, Vol. 4, No. 8, pp. 8866–8873, (2017).
- [138] J. Wang, R. Fu, Y. Li and J. Zhang, "Effects of deep cryogenic treatment and low-temperature aging on the mechanical properties of friction-stir-welded joints of 2024-T351 aluminum alloy," *Mater. Sci. Eng. A*, Vol. 609, No. 1, pp. 147–153, (2014).
- [139] Y. Wang, R. Fu, L. Jing, Y. Li and D. Sang, "Grain refinement and nanostructure formation in pure copper during cryogenic friction stir processing," *Mater. Sci. Eng. A*, Vol. 703, No. 1, pp. 470–476, (2017).
- [140] D. Zhemchuzhnikova, S. Malopheyev, S. Mironov and R. Kaibyshev, "Cryogenic properties of Al-Mg-Sc-Zr friction-stir welds," *Mater. Sci. Eng. A*, Vol. 598, No. 1, pp. 387–395, (2014).
- [141] N. Ferreira, J. S. Jesus, J. A. M. Ferreira, C. Capela, J. M. Costa and A. C. Batista,



- “Effect of bead characteristics on the fatigue life of shot peened Al 7475-T7351 specimens,” *Int. J. Fatigue*, Vol. 134, No. 105521, (2020).
- [142] P. Liu, S. Sun and J. Hu, “Effect of laser shock peening on the microstructure and corrosion resistance in the surface of weld nugget zone and heat-affected zone of FSW joints of 7050 Al alloy,” *Opt. Laser Technol.*, Vol. 112, No. 1, pp. 1–7, (2019).
- [143] Y. Sano, K. Masaki, T. Gushi and T. Sano, “Improvement in fatigue performance of friction stir welded A6061-T6 aluminum alloy by laser peening without coating,” *Mater. Des.*, Vol. 36, No. 1, pp. 809–814, (2012).
- [144] M. H. Shojaeefard, A. Khalkhali, M. Akbari and P. Asadi, “Investigation of friction stir welding tool parameters using FEM and neural network,” *Proc. Inst. Mech. Eng. Part L J. Mater. Des. Appl.*, Vol. 229, No. 3, pp. 209–217, (2015).
- [145] D. Devaiah, K. Kishore and P. Laxminarayana, “Optimal FSW process parameters for dissimilar aluminium alloys (AA5083 and AA6061) Using Taguchi Technique,” *Mater. Today Proc.*, Vol. 5, No. 2, pp. 4607–4614, (2018).
- [146] M. W. Dewan, D. J. Huggett, T. Warren Liao, M. A. Wahab and A. M. Okeil, “Prediction of tensile strength of friction stir weld joints with adaptive neuro-fuzzy inference system (ANFIS) and neural network,” *Mater. Des.*, Vol. 92, No. 1, pp. 288–299, (2016).
- [147] R. Teimouri and H. Baseri, “Forward and backward predictions of the friction stir welding parameters using fuzzy-artificial bee colony-imperialist competitive algorithm systems,” *J. Intell. Manuf.*, Vol. 26, No. 2, pp. 307–319, (2015).
- [148] N. F. Alkayem, B. Parida, and S. Pal, “Optimization of friction stir welding process parameters using soft computing techniques,” *Soft Comput.*, Vol. 21, No. 23, pp. 7083–7098, (2017).
- [149] R. Padmanaban, V. Balusamy, V. Saikrishna and K. Gopath Niranthar, “Simulated annealing based parameter optimization for Friction Stir Welding of dissimilar aluminum alloys,” *Procedia Eng.*, Vol. 97, No. 1, pp. 864–870, (2014).
- [150] S. K. Gupta, K. N. Pandey and R. Kumar, “Artificial intelligence-based modelling and multi-objective optimization of friction stir welding of dissimilar AA5083-O and AA6063-T6 aluminium alloys,” *Proc. Inst. Mech. Eng. Part L J. Mater. Des. Appl.*, vol. 232, No. 4, pp. 333–342, (2018).
- [151] T. A. Shehabeldeen, J. Zhou, X. Shen, Y. Yin and X. Ji, “Comparison of RSM with ANFIS in predicting tensile strength of dissimilar friction stir welded AA2024 - AA5083 aluminium alloys,” *Procedia Manuf.*, Vol. 37, No. 1, pp. 555–562, (2019).
- [152] N. Rajamanickam, V. Balusamy, P. R. Thyla and G. H. Vignesh, “Numerical simulation of thermal history and residual stresses in friction stir welding of Al 2014-T6,” *J. Sci. Ind. Res. (India)*, Vol. 68, No. 3, pp. 192–198, (2009).
- [153] H. W. Zhang, Z. Zhang, and J. T. Chen, “The finite element simulation of the friction stir welding process,” *Mater. Sci. Eng. A*, Vol. 403, No. 1–2, pp. 340–348, (2005).
- [154] L. Long, G. Chen, S. Zhang, T. Liu and Q. Shi, “Finite-element analysis of the tool tilt angle effect on the formation of friction stir welds,” *J. Manuf. Process.*, Vol. 30, pp. 562–569, (2017).
- [155] P. V. Chandra Sekhara Rao, E. Mounika and G. Vikram, “Process parameters optimization on FSW of Polycarbonate and AA6061,” *Mater. Today Proc.*, Vol. 19, No. 2, pp. 637–641, (2019).
- [156] N. A. Muhammad, C. S. Wu and W. Tian, “Effect of ultrasonic vibration on the intermetallic compound layer formation in Al/Cu friction stir weld joints,” *J. Alloys Compd.*, Vol. 785, No. 1, pp. 512–522, (2019).
- [157] M. Ambekar and J. Kittur, “Multiresponse optimization of friction stir welding process parameters by an integrated WPCA-ANN-PSO approach,” *Mater. Today Proc.*, Vol. 27, No. 1, pp. 363–368, (2020).

- [158] B. S. Taysom, C. D. Sorensen and J. D. Hedengren, "Dynamic modeling of friction stir welding for model predictive control," *J. Manuf. Process.*, Vol. 23, No. 1, pp. 165–174, (2016).
- [159] G. Chen *et al.*, "Effects of pin thread on the in-process material flow behavior during friction stir welding: A computational fluid dynamics study," *Int. J. Mach. Tools Manuf.*, Vol. 124, No. 1, pp. 12–21, (2018).
- [160] S. Sree Sabari, S. Malarvizhi, V. Balasubramanian and G. Madusudhan Reddy, "Experimental and numerical investigation on under-water friction stir welding of armour grade AA2519-T87 aluminium alloy," *Def. Technol.*, Vol. 12, No. 4, pp. 324–333, (2016).
- [161] J. H. Kim, D. S. Jo and B. M. Kim, "Hardness prediction of weldment in friction stir welding of AA6061 based on numerical approach," *Procedia Eng.*, Vol. 207, No. 1, pp. 586–590, (2017).
- [162] S. Zhang *et al.*, "Numerical analysis and analytical modeling of the spatial distribution of heat flux during friction stir welding," *J. Manuf. Process.*, Vol. 33, No. 1, pp. 245–255, (2018).
- [163] R. Rzaev, A. Dzhalukhambetov, A. Chularis and A. Valisheva, "Mathematical Modeling of Process of the Friction Stir Welding," *Mater. Today Proc.*, Vol. 11 No. 1, pp. 591–599, (2019).
- [164] S. Sudhagar, M. Sakthivel, P. J. Mathew and S. A. A. Daniel, "A multi criteria decision making approach for process improvement in friction stir welding of aluminium alloy," *Meas. J. Int. Meas. Confed.*, Vol. 108, No. 1, pp. 1–8, (2017).
- [165] A. Heidarzadeh, S. Mironov, R. Kaibyshev, G. Cam, A. Simar, A. Gerlich, F. Khodabakhshi, A. Mostafaei, D. P. Field, J. D. Robson, A. Deschamps and P. J. Withers, "Friction stir welding/processing of metals and alloys: A comprehensive review on microstructural evolution," *Prog. Mater. Sci.*, No. 100752, (2020).
- [166] X. Meng, Y. Huang, J. Cao, J. Shen and J. F. Dos Santos, "Recent progress on control strategies for inherent issues in friction stir welding," *Progress in Materials Science*, Volume 115, No. 100706, (2021).
- [167] R. S. Mishra and Z. Y. Ma, "Friction stir welding and processing, *Materials Science and Engineering: R: Reports*," Vol. 50, No. 1–2, pp. 1-78, (2005).

Copyrights ©2021 The author(s). This is an open access article distributed under the terms of the Creative Commons Attribution (CC BY 4.0), which permits unrestricted use, distribution, and reproduction in any medium, as long as the original authors and source are cited. No permission is required from the authors or the publishers.



### How to cite this paper:

Satish Chinchani and Vaibhav S. Gaikwad, "State of the art in friction stir welding and ultrasonic vibration-assisted friction stir welding of similar/dissimilar aluminum alloys," *J. Comput. Appl. Res. Mech. Eng.*, Vol. 11, No. 1, pp. 67-100, (2021).

**DOI:** 10.22061/JCARME.2021.7390.1983

**URL:** [https://jcarme.sru.ac.ir/?\\_action=showPDF&article=1533](https://jcarme.sru.ac.ir/?_action=showPDF&article=1533)

